UNIVERSITY OF THESSALY
SCHOOL OF ENGINEERING
DEPARTMENT OF MECHANICAL ENGINEERING

Diploma Thesis

Elastic Beam Analysis: Analytical and Numerical solutions

by

IOANNIS SIOMADIS

SUBMITTED IN PARTIAL FULFILMENT OF THE
REQUIREMENTS FOR DIPLOMA IN MECHANICAL ENGINEERING
2022

The approval of the Diploma Thesis by the Department of Mechanical Engineering, School of Engineering, University of Thessaly does not imply acceptance of the author's views (N. 5343/32 $\alpha\rho$. 202 $\pi\alpha\rho$. 2).

Approved by the Three Members of the Advisory Committee:

First Member (Supervisor)

Professor Nikolaos Aravas
Department of Mechanical Engineering, University of Thessaly

Second Member

Assistant Professor Michalis Agoras
Department of Mechanical Engineering, University of Thessaly

Third Member

Dr. Ioanna Papadioti
Department of Mechanical Engineering, University of Thessaly

Abstract

Elastic Beam Analysis: Analytical and Numerical solutions

Ioannis Siomadis

Supervisor: Professor N. Aravas

The beam is arguably one of the most essential structural elements, widely used in civil and mechanical engineering applications of any field, in one form or another. Therefore, it is extremely important for engineers to possess the appropriate methods to be in a position to effectively and accurately estimate the stress field of a beam that is subjected to specific loading. This work is concerned with the implementation of analytical and computational methods with the purpose of calculating the stress distribution in a bent beam with rectangular cross section. In most cases of a bent beam analysis, the main priority is to determine the normal stresses, due to the scale of their magnitude. However, the primary focus of this thesis is to study the distribution of shear stresses on the beam in relation to the geometric characteristics of the rectangular cross section. The analytical solution of the problem is derived through the application of Saint Venant's method of elastic beam analysis, while the numerical analysis is carried out with the ABAQUS/Standard solver, provided by general purpose finite element software ABAQUS.

Keywords: Bending; Saint Venant Beams; Finite Element Method;

Acknowledgements

First of all, I would like to thank Professor Nikolaos Aravas, for assigning and supervising this thesis subject, which served as a great opportunity for me to expand my knowledge in the field of Mechanics of Materials and Computational Mechanics.

I would also like to thank PhD student Socrates Xenos for his help and guidance throughout this project.

Most importantly, I need to thank my family for supporting me throughout all the years of my studies.

Contents

List of Figures

List of Tables

Introduction

The beam is one of the most essential structural elements found in most civil and mechanical engineering applications. Therefore, is very important for designers to be able to determine the stress and strain fields developed in beams, with adequate accuracy. To achieve this goal, a number of approaches can be employed, including analytical, approximate and numerical methods.

The problem of a prismatic beam subjected to various types of loads has been widely studied and discussed from both the analytical and numerical point of view. *Saint Venant's method* of analyzing linear elastic isotropic beams is one of the most well known in literature and still serves as a good reference model for engineers to evaluate stress and strain fields. Despite its significant limitation, concerning the application of the loads strictly in the bases of the beam and not the lateral surface, the method can provide valuable results in the problems of extension, torsion, flexure and bending of the beam with shear forces (I.S. Sokolnikoff [6], N.Aravas [4]). As far as computational methods are concerned, the *Finite Element Method* has been proved to be a very effective procedure to solve the governing equations (equilibrium, kinematic, constitutive) and extract reliable results, in the field of Solid Mechanics.

In the context of this thesis, Saint Venant's method will be used to obtain an exact solution of the stress field of a bent beam with rectangular cross section subjected to transverse shear forces and study the effects of its geometry on the location, magnitude and direction of the maximum shear stress. The finite element method is applied on a statically equivalent cantilever beam in order to compare and verify the numerical results with the exact solution, and its implementation is accomplished through commercial FEA software ABAQUS.

Chapter 1 is a brief review of the Theory of Elasticity, containing a presentation of the constitutive equations and the formulation of the boundary value problem of elastostatics. Chapter 2 consists of an introduction to Saint Venant's method and an application on bent beams with rectangular cross section. Finally, Chapter 3 includes a description of the procedure followed to implement the finite element method using ABAQUS, as well as a showcase and discussion of the numerical results in comparison to the analytical solution.

Standard notation is used throughout this thesis. Boldface symbols denote tensors the order of which is indicated by the context. The tensor components are written with respect to a fixed Cartesian coordinate system with base vectors $\boldsymbol{e}_i$ (i=1,2,3), and the summation convention is used for repeated Latin indices. The superscript (-1) is used to denote the inverse of a tensor and δ_{ij} is used for the Kronecker delta. Generally, boldface lowercase letters (e.g. $\mathbf{a, b}$) are used for vectors, boldface capital letters (e.g. $\mathbf{A, B}$) are used for second order tensors and boldface caligraphic capital letters (e.g. $\boldsymbol{\mathcal{A}}$, $\boldsymbol{\mathcal{B}}$) are used for fourth order tensors.

Chapter 1

Theory of Elasticity

This chapter, is a review of the fundamental theoretical background that is relevant to the work done in the present thesis. More specifically, it consists of a discussion on Linear Elastic Materials and the Boundary Value problem of Elastostatics.

1.1 Linear Elastic Bodies

This section pertains to the properties of the material considered in this thesis as well as the stress-strain relations in a material point, which are referred to as *constitutive equations* and occur as a result of those properties. In general, the σ_{ij} components of the stress tensor in a material point depend on all the ε_{ij} components of the strain tensor, the temperature T, the 'history' (meaning the past values) of strains and other factors (such as humidity, porosity etc.). The material involved in this work is considered to be such that the value of the stress tensor at a specified material point depends on the value of the strain tensor at that point, while it is completely independent from the values of $\boldsymbol{\varepsilon}$ at the rest of the body. This hypothesis leads to the so-called *local* continuum theories and the corresponding materials which are characterized as *simple*. Furthermore, the material under examination is considered to be *linear elastic*, which means that the σ_{ij} components of the stress tensor are linear functions of the ε_{ij} components of the strain tensor.

1.1.1 Linear Elastic Materials

It has been shown through experiments that the length and angular deformations of structural materials change *linearly* with the imposed stresses, assuming that the stresses do not surpass a certain limit. Also, when the stresses are removed those deformations are nullified and the material returns to its original state, meaning there is no macroscopic proof that the material has been previously loaded. In this case, the material behavior is *linear elastic*.

The main characteristic of elastic behavior is that the material returns to its original state when the stresses are removed. It is worth noting that metals are linear elastic when the

magnitude of the stresses is such that it would not cause plastic deformations, while there are materials, such as caoutchouc, which may be elastic at all stress levels but the stress-strain relation is non-linear (Figure 1.1).

(a) Linear elastic   (b) Nonlinear elastic   (c) Inelastic
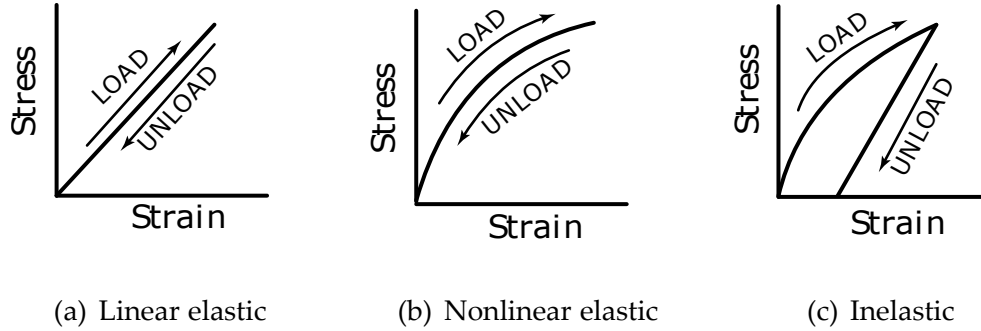
Figure 1.1: Different types of material behavior.

Considering a *simple elastic* (linear on non-linear) material for which the stress tensor $\boldsymbol{\sigma}$ at a material point $\mathbf{X}$[1] depends solely on the value of strain tensor $\boldsymbol{\varepsilon}$ at that point, the general form of the constitutive equation is

$$\boldsymbol{\sigma}(X) = \boldsymbol{f}(\varepsilon(X), X) \tag{1.1}$$

where $\boldsymbol{f}$ is second order tensor function. Equation (1.1) states that the stress $\boldsymbol{\sigma}$ at the point $\mathbf{X}$ of a body depends on the value of $\boldsymbol{\varepsilon}$ at that point and its location, $\mathbf{X}$. If the mechanical properties of the material are the same at every point, the material is characterized as *homogeneous*, $\boldsymbol{f}$ is independent of $\mathbf{X}$ and as a result the constitutive equation becomes

$$\boldsymbol{\sigma}(X) = \boldsymbol{f}(\varepsilon(X)) \qquad \text{or simply} \qquad \boldsymbol{\sigma}(X) = \boldsymbol{f}(\varepsilon) \tag{1.2}$$

which means that the stress-strain relation is the same at every point of the body. The materials examined in this thesis are considered to be *homogenous.*

1.1.2 Elastic Tensors

In the special case of *linear* elastic materials $\boldsymbol{f}$ is a linear function of $\boldsymbol{\varepsilon}$, meaning that the σ_{ij} components of the stress tensor are linear functions of the ε_{ij} components of the strain tensor and the general form of the constitutive equations using tensor and index notation is

$$\boldsymbol{\sigma} = \boldsymbol{\mathcal{L}} : \boldsymbol{\varepsilon} \qquad \text{and} \qquad \sigma_{ij} = \mathcal{L}_{ijkl}\varepsilon_{kl} \tag{1.3}$$

---

[1]vector $\mathbf{X}$, commonly used in continuum mechanics theories, is the position vector in a cartesian coordinate system used to denote any material point of the body.

The 81 $\mathcal{L}_{ijkl}$ coefficients express the properties of the material in the directions of the axis system based on which the components σ_{ij} and ε_{ij} are evaluated. These coefficients are called *elastic constants* and have stress dimensions.

Since the stress and strain tensors are symmetric, eq.(1.3) defines six independent linear equations, which can be solved for the components ε_{ij} of the strain tensor and as a result the constitutive equations would have the form shown below

$$\boldsymbol{\varepsilon} = \boldsymbol{\mathcal{M}} : \boldsymbol{\sigma} \qquad \text{and} \qquad \varepsilon_{ij} = \mathcal{M}_{ijkl}\sigma_{kl} \tag{1.4}$$

where the coefficients $\mathcal{M}_{ijkl}$ have dimensions of $(stress)^{-1}$.

The quantities σ_{ij} and ε_{ij} are the components of second order tensors. Therefore, based on equations (1.3) and (1.4), it can be concluded that $\mathcal{L}_{ijkl}$ and $\mathcal{M}_{ijkl}$ are components of fourth order tensors $\boldsymbol{\mathcal{L}}$ and $\boldsymbol{\mathcal{M}}$ respectively. $\boldsymbol{\mathcal{L}}$ is known as the *elasticity* tensor, while $\boldsymbol{\mathcal{M}}$ is known as the *compliance* tensor.

1.1.3 Elastic Tensor Symmetries

Due to the symmetry of tensors $\boldsymbol{\sigma}$ and $\boldsymbol{\varepsilon}$ and equations (1.3) and (1.4), tensors $\boldsymbol{\mathcal{L}}$ and $\boldsymbol{\mathcal{M}}$ are symmetric to the first two indices. Additionally, it can be shown that the elastic tensors are symmetric to the third and fourth indices, therefore its

$$\boxed{\mathcal{L}_{ijkl} = \mathcal{L}_{jikl} = \mathcal{L}_{ijlk}} \qquad \text{and} \qquad \boxed{\mathcal{M}_{ijkl} = \mathcal{M}_{jikl} = \mathcal{M}_{ijlk}} \tag{1.5}$$

Theses symmetries are known in literature as the *'minor symmetries'* of elastic tensors and they reduce the number of independent elastic coefficients from 81 to 36.

Furthermore, in can be shown that in the case of *'hyperelastic'*[2] materials the elastic tensors are symmetric to the pairs (i, j) and (k, l), so its

$$\boxed{\mathcal{L}_{ijkl} = \mathcal{L}_{klij}} \qquad \text{and} \qquad \boxed{\mathcal{M}_{ijkl} = \mathcal{M}_{klij}} \tag{1.6}$$

These symmetries are known as *'major symmetries'* and they further reduce the number of independent elastic constants from 36 to 21.

From this point onwards, the materials examined in this thesis are considered to be linear hyperelastic, but in short will be simply called *linear elastic*.

1.1.4 Matrix form of linear elastic equations

The constitutive equations (1.3) and (1.4) can written in matrix form as shown below

$$\{\hat{\sigma}\} = [\hat{\mathcal{L}}]\{\hat{\varepsilon}\}, \qquad \{\hat{\varepsilon}\} = [\hat{\mathcal{M}}]\{\hat{\sigma}\}, \qquad [\hat{\mathcal{M}}] = [\hat{\mathcal{L}}]^{-1} \tag{1.7}$$

---

[2]a material is characterized as hyperelastic when the total work performed by the imposed loads in a cycle of loading-unloading is zero.

where

$$
\{\hat{\sigma}\} = \begin{Bmatrix} \sigma_{11} \\ \sigma_{22} \\ \sigma_{33} \\ \sqrt{2}\sigma_{23} \\ \sqrt{2}\sigma_{13} \\ \sqrt{2}\sigma_{12} \end{Bmatrix}, \qquad \{\hat{\varepsilon}\} = \begin{Bmatrix} \varepsilon_{11} \\ \varepsilon_{22} \\ \varepsilon_{33} \\ \sqrt{2}\varepsilon_{23} \\ \sqrt{2}\varepsilon_{13} \\ \sqrt{2}\varepsilon_{12} \end{Bmatrix}, \tag{1.8}
$$

$$
[\hat{\mathcal{L}}] = \begin{bmatrix} \mathcal{L}_{1111} & \mathcal{L}_{1122} & \mathcal{L}_{1133} & \sqrt{2}\mathcal{L}_{1123} & \sqrt{2}\mathcal{L}_{1113} & \sqrt{2}\mathcal{L}_{1112} \\ & \mathcal{L}_{2222} & \mathcal{L}_{2233} & \sqrt{2}\mathcal{L}_{2223} & \sqrt{2}\mathcal{L}_{2213} & \sqrt{2}\mathcal{L}_{2212} \\ & & \mathcal{L}_{3333} & \sqrt{2}\mathcal{L}_{3323} & \sqrt{2}\mathcal{L}_{3313} & \sqrt{2}\mathcal{L}_{3312} \\ & & & 2\mathcal{L}_{2323} & 2\mathcal{L}_{2313} & 2\mathcal{L}_{2312} \\ & symm & & & 2\mathcal{L}_{1313} & 2\mathcal{L}_{1312} \\ & & & & & 2\mathcal{L}_{1212} \end{bmatrix}, \tag{1.9}
$$

and

$$
[\hat{\mathcal{M}}] = [\hat{\mathcal{L}}]^{-1} = \begin{bmatrix} \mathcal{M}_{1111} & \mathcal{M}_{1122} & \mathcal{M}_{1133} & \sqrt{2}\mathcal{M}_{1123} & \sqrt{2}\mathcal{M}_{1113} & \sqrt{2}\mathcal{M}_{1112} \\ & \mathcal{M}_{2222} & \mathcal{M}_{2233} & \sqrt{2}\mathcal{M}_{2223} & \sqrt{2}\mathcal{M}_{2213} & \sqrt{2}\mathcal{M}_{2212} \\ & & \mathcal{M}_{3333} & \sqrt{2}\mathcal{M}_{3323} & \sqrt{2}\mathcal{M}_{3313} & \sqrt{2}\mathcal{M}_{3312} \\ & & & 2\mathcal{M}_{2323} & 2\mathcal{M}_{2313} & 2\mathcal{M}_{2312} \\ & symm & & & 2\mathcal{M}_{1313} & 2\mathcal{M}_{1312} \\ & & & & & 2\mathcal{M}_{1212} \end{bmatrix}. \tag{1.10}
$$

In the expressions shown above, the symbol ($\hat{\bullet}$) denotes the matrix form of the quantity it is used on. This form of the stress, strain and elastic tensors facilitates the matrix representation of tensor products that are commonly found in calculations.

1.1.5 Isotropic linear elastic materials

A particular category of linear elastic materials, includes materials that display identical properties in all directions at any given point (there is no characteristic orientation). Those materials are known as *isotropic*. The elastic tensors of isotropic materials have 12 non-zero components. There is a variety of elastic constants used in literature such as the modulus of elasticity (Young's modulus) E, the Poisson ration ν, the shear modulus G and the bulk modulus κ. It is essential to mention that only 2 of those constants are independent, meaning that if 2 of those quantities are known (through an experiment for instance) the material properties can be fully determined.

It is also important to have an understanding of the physical meaning of the elastic constants,

especially the most commonly used ones, E and ν. A physical interpretation of these constants as well as the relations between them (given the fact that they are not independent) is shown below:

- *Young's modulus E* is the slope of the stress-strain curve in uniaxial tension ($E \equiv \frac{\sigma}{\varepsilon}$). It has dimensions of stress (e.g. for steel $E \sim 200 GPa$) and it can be interpreted as a measure of the stiffness of the material. The larger the value of E, the stiffer the material.

- *Poisson's ratio ν* is the ratio of lateral to longitudinal strain in uniaxial tension ($E \equiv \frac{|\varepsilon_{22}|}{|\varepsilon_{11}|} = \frac{|\varepsilon_{33}|}{|\varepsilon_{11}|}$). It is dimensionless and typically ranges from 0.2-0.5 (for most metals it is around 0.3). If $\nu = 0.5$, the material is called *incompressible* and its volume remains the same, no matter how it is deformed (volumetric strain$\rightarrow \varepsilon_{kk} = 0$).

- *Shear modulus G* quantifies the material's resistance to shear deformations and has dimensions of stress.

$$G = \frac{E}{2(1+\nu)} \tag{1.11}$$

- *Shear modulus κ* quantifies the material's resistance to volume changes ($\kappa \equiv \frac{p}{\varepsilon_{ii}}$, where $p = \sigma_{kk}/3$ is the hydrostatic stress).

$$\kappa = \frac{E}{3(1-2\nu)} = \frac{2}{3}\frac{1+\nu}{1-2\nu}G = \frac{GE}{3(3G-E)} \tag{1.12}$$

Another noteworthy pair of elastic constants commonly found in literature are the *Lamé constants*, λ and μ. The relations between the Lamé constants and the constants E, ν, G and κ are the following:

$$\mu = G = \frac{E}{2(1+\nu)} = \frac{3}{2}\frac{1-2\nu}{1+\nu}\kappa , \tag{1.13}$$

and

$$\lambda = \frac{2\nu}{1-2\nu}G = \frac{\nu}{(1+\nu)(1-2\nu)}E = \frac{3\nu}{1+\nu}\kappa = \kappa - \frac{2}{3}G . \tag{1.14}$$

In the case of isotropic linear elastic materials the elasticity and compliance tensors, shown in equations (1.9) and (1.10) respectively, take the following matrix form:

$$[\hat{\mathcal{L}}] = \frac{E}{(1+\nu)(1-2\nu)}\begin{bmatrix} 1-\nu & \nu & \nu & 0 & 0 & 0 \\ & 1-\nu & \nu & 0 & 0 & 0 \\ & & 1-\nu & 0 & 0 & 0 \\ & & & 1-2\nu & 0 & 0 \\ & symm & & & 1-2\nu & 0 \\ & & & & & 1-2\nu \end{bmatrix} \tag{1.15}$$

and

$$[\hat{\mathcal{M}}] = [\hat{\mathcal{L}}]^{-1} = \frac{1}{E} \begin{bmatrix} 1 & -\nu & -\nu & 0 & 0 & 0 \\ & 1 & -\nu & 0 & 0 & 0 \\ & & 1 & 0 & 0 & 0 \\ & & & 1+\nu & 0 & 0 \\ & symm & & & 1+\nu & 0 \\ & & & & & 1+\nu \end{bmatrix}. \tag{1.16}$$

Using index notation the elastic tensors can be written as:

$$\boxed{\mathcal{L}_{ijkl} = G(\delta_{ik}\delta_{jl} + \delta_{il}\delta_{jk}) + \left(\kappa - \frac{2}{3}G\right)\delta_{ij}\delta_{kl}} \tag{1.17}$$

and

$$\boxed{\mathcal{M}_{ijkl} = \frac{1}{4G}(\delta_{ik}\delta_{jl} + \delta_{il}\delta_{jk}) + \frac{1}{3}\left(\frac{1}{3\kappa} - \frac{1}{2G}\right)\delta_{ij}\delta_{kl}}. \tag{1.18}$$

Finally, using tensor notation it is

$$\boxed{\mathcal{L} = 2G\mathcal{K} + 3\kappa\mathcal{J}} \qquad \text{and} \qquad \boxed{\mathcal{M} = \frac{1}{2G}\mathcal{K} + \frac{1}{3\kappa}\mathcal{J}} \tag{1.19}$$

with $\mathcal{K} = \mathcal{I} - \mathcal{J}$, where $\mathcal{I}$, $\mathcal{J}$ and $\mathcal{K}$ are the identity 4th order tensors in the subspace of the symmetric, spherical and deviatoric tensors respectively, with components:

$$\mathcal{K}_{ijkl} = \mathcal{I}_{ijkl} - \mathcal{J}_{ijkl}, \qquad \mathcal{I}_{ijkl} = \frac{1}{2}(\delta_{ik}\delta_{jl} + \delta_{il}\delta_{jk}), \qquad \mathcal{J}_{ijkl} = \frac{1}{3}\delta_{ij}\delta_{kl} . \tag{1.20}$$

1.2 The Boundary Value Problem of Elastostatics

This section is a brief discussion on the equations and appropriate boundary conditions required to formulate the boundary value problem which must be solved in order to determine the displacements, strains and stresses of a linear elastic body.

1.2.1 Field equations

The governing equations of a linear elastic body $\mathbb{B}$:

equilibrium equations: $\qquad \boldsymbol{\nabla} \cdot \boldsymbol{\sigma} + \rho\boldsymbol{b} = \boldsymbol{0} \qquad \text{or} \qquad \sigma_{ij,j} + \rho b_i = 0, \tag{1.21}$

kinematic equations: $\qquad \boldsymbol{\varepsilon} = \frac{1}{2}(\boldsymbol{u}\overleftarrow{\boldsymbol{\nabla}} + \boldsymbol{\nabla}\boldsymbol{u}) \qquad \text{or} \qquad \varepsilon_{ij} = \frac{1}{2}(u_{i,j} + u_{j,i}), \tag{1.22}$

constitutive equations: $\quad\quad \boldsymbol{\sigma} = \boldsymbol{\mathcal{L}} : \boldsymbol{\varepsilon} \quad$ or $\quad \sigma_{ij} = \mathcal{L}_{ijkl}\varepsilon_{ij}.$ $\quad\quad$ (1.23)

Should be noted that the index $_{,i}$ indicates partial differentiation with respect to X_i ($u_{j,i} = \partial u_j/\partial X_i$), the indices $_{,ij}$ indicate partial differentiation with respect to X_i and X_j ($u_{k,ij} = \partial^2 u_k/\partial X_i \partial X_j$) etc.

In the above equations $\boldsymbol{u}$ is the displacement vector, $\boldsymbol{\varepsilon}$ is the strain tensor, $\boldsymbol{\sigma}$ is the stress tensor, ρ is the mass density, $\boldsymbol{b}$ are the applied body forces and $\boldsymbol{\mathcal{L}}$ is the elasticity tensor of the material, where $\boldsymbol{\mathcal{L}}$, ρ and $\boldsymbol{b}$ are known quantities.

Equations (1.21), (1.22) and (1.23) define 15 scalar equations: three equilibrium equations, six kinematic equations ($\boldsymbol{\varepsilon}$-$\boldsymbol{u}$ relations) and six constitutive equations. Nine of those are partial defferential equations ((1.21) and (1.22)) and the rest are algebraic equations (1.23).

The unknowns of the problem are also 15: the three u_{ij} components of displacement vector $\boldsymbol{u}$, the six ε_{ij} components of the symmetric strain tensor $\boldsymbol{\varepsilon}$ and the six σ_{ij} components of the stress tensor $\boldsymbol{\sigma}$.

It is important to note that the equilibrium and the kinematic equations are applicable to any material under examination, not just linear elastic materials. On the contrary, the constitutive equations are valid only in the case of linear elastic materials.

1.2.2 Boundary Conditions

The field equations stated in the previous section are completed with the addition of the boundary conditions, which describe the applied surface loads, the applied surface displacements and the supports of the body.

The boundary conditions on the boundary $\partial\mathbb{B}$ of the body are

$$\boldsymbol{u} = \hat{\boldsymbol{u}} \quad\quad \text{or} \quad\quad u_i = \hat{u}_i \quad\quad \text{in} \quad\quad \partial\mathbb{B}_u, \quad\quad (1.24)$$

$$\boldsymbol{\sigma} \cdot \boldsymbol{n} = \hat{\boldsymbol{t}} \quad\quad \text{or} \quad\quad \sigma_{ij}n_j = \hat{t}_i \quad\quad \text{in} \quad\quad \partial\mathbb{B}_t, \quad\quad (1.25)$$

where $\boldsymbol{n}$ is the unit vector normal to $\partial\mathbb{B}$ and pointing outside of the body $\mathbb{B}$, $\hat{\boldsymbol{u}}$ are the applied (known) displacements in the $\partial\mathbb{B}_u$ portion of the boundary and $\hat{\boldsymbol{t}}$ are the applied (known) surface loads in the $\partial\mathbb{B}_t$ portion of the boundary ($\partial\mathbb{B}_u \cup \partial\mathbb{B}_t = \partial\mathbb{B}$ and $\partial\mathbb{B}_u \cap \partial\mathbb{B}_t = \varnothing$). According to the above boundary conditions, either the displacement $\boldsymbol{u}$ or the stress vector $\boldsymbol{\sigma} \cdot \boldsymbol{n}$ is known at any point of the boundary $\partial\mathbb{B}$. It should also be noted that the portions $\partial\mathbb{B}_u$ and $\partial\mathbb{B}_t$ of the boundary are complementary and not overlapping. This means that it is impossible to simultaneously define both the displacement $\boldsymbol{u}$ and the stress vector $\boldsymbol{\sigma} \cdot \boldsymbol{n}$ at any point of the boundary $\partial\mathbb{B}$.

The first kind of boundary conditions (eq. 1.24) includes those points of the boundary $\partial\mathbb{B}$ on which displacements ($\hat{\boldsymbol{u}} \neq \boldsymbol{0}$) or supports ($\hat{\boldsymbol{u}} = \boldsymbol{0}$) are imposed. The second kind (eq. 1.25) includes regions where surface loads $\hat{\boldsymbol{t}}$ are imposed and non-loaded areas where $\hat{\boldsymbol{t}} = \boldsymbol{0}$.

In certain problems it is possible to have a third kind of boundary conditions, in a portion $\partial\mathbb{B}_{ut}$ of the boundary, which define the component of $\boldsymbol{u}$ (or $\boldsymbol{\sigma}\cdot\boldsymbol{n}$) normal to the boundary $\partial\mathbb{B}$ and the component of $\boldsymbol{\sigma}\cdot\boldsymbol{n}$ (or $\boldsymbol{u}$) tangent to $\partial\mathbb{B}$. In this case, the boundary is divided to the non-overlapping parts $\partial\mathbb{B}_u$, $\partial\mathbb{B}_t$ and $\partial\mathbb{B}_{ut}$.

1.2.3 Saint Venant's Principle

In order to obtain an exact solution for the Boundary Value problem of Elastostatics, presented in the previous paragraphs, the application of analytical methods is required to solve the system of differential and algebraic equations for $\boldsymbol{u}$, $\boldsymbol{\varepsilon}$ and $\boldsymbol{\sigma}$. In many practical problems, this course of action leads to no result, as it is impossible to solve the problem with common analytical procedures used in mathematics. However, there are certain occasions where an analytical solution can be obtained for a 'similar' problem. In this problem, the body remains the same, but some of the boundary conditions are being replaced with different, statically equivalent ones, in the sense that they result in the same net force and moment. According to *Saint Venant's principle*, the effect of this change of boundary conditions is 'local'. This means that in locations 'far enough' from the region of the boundary where the boundary condition change took place, the solutions of the original and the slightly modified problem are roughly the same. A review of the available literature on the topic until 1989 was presented by Horgan.

Saint Venant's principle is exceptionally important, as it allows for an approximate solution to be obtained in problems that were normally impossible to solve analytically, using regular mathematical procedures.

Chapter 2

Saint Venant Beams

This chapter is a presentation of the formulation of what is known in literature as *'Saint Venant beams'*, a theory which pertains to obtaining the stress distribution on a beam which is only loaded on its bases, while the lateral surface remains free of external loads.

2.1 Problem Geometry

The Saint Venant beam is geometrically defined by a prismatic surface, which is generated by parallel lines, and the two bases vertical to the lateral prismatic surface (Figure 2.1). In this section (x, y, z) are used instead of the Cartesian coordinated (X_1, X_2, X_3), hence $u_x = u_1$, $\varepsilon_{xx} = \varepsilon_{11}$, $\sigma_{xy} = \sigma_{12}$ etc. for the components of the displacement vector, the strain tensor and the stress tensor. The x-axis of the x-y-z system of coordinates used, is parallel to the lines that generate the lateral surface of the beam and the unit base vectors of this system are noted as $(\boldsymbol{e}_x, \boldsymbol{e}_y, \boldsymbol{e}_z)$. The section surface of the beam and a plane vertical to the x-axis, defines the cross section of the beam.
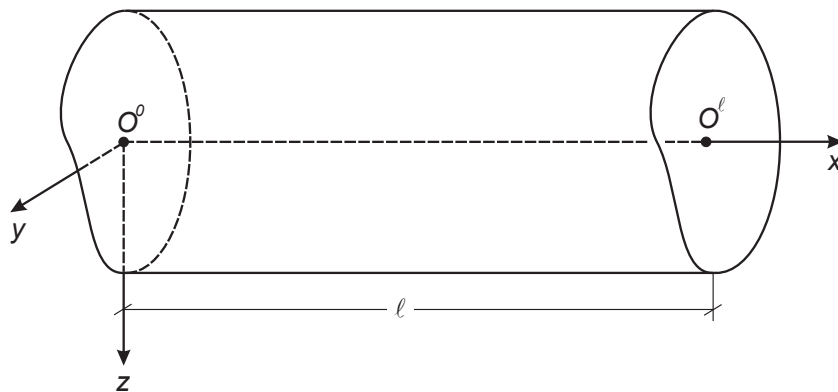

Figure 2.1: Schematic representation of the beam.

The beam is uniform in the longitudinal x-direction, can be solid or hollow (cross section

with holes) and its length is ℓ. One of the two bases is located in the $x = 0$ plane and the other in the $x = \ell$ plane. The symbol O^0 is used to denote the origin of the coordinates system in the $x = 0$ base. The location of O^0 in the $x = 0$ plane is generally arbitrary. However, in certain problems, O^0 is set on the geometric center of the $x = 0$ base, so that the x-axis crosses the geometric centers of the cross sections. In these cases, the coordinate system is referred to as *'central'* and it is

$$\int_\Omega y \, dA = \int_\Omega z \, dA = 0 \qquad \text{in every cross section,} \tag{2.1}$$

where Ω is the surface of the cross section. The orientation of the y and z axis on the $x = 0$ plane is also arbitrary. In some problems though, the orientation of y and z is chosen so that the 'centrifugal area moment of inertia', I_{yz} becomes zero:

$$I_{yz} \equiv \int_\Omega y \, z \, dA = 0. \tag{2.2}$$

In this case, the axis system is called *'central and principal'*.
The external surface of the beam consists of the two bases (the two cross sections at $x = 0$ and $x = \ell$) and the lateral surface. The lateral surface remains free of loads and there are no body forces applied on the beam. Loads can only be applied in the bases $x = 0$ and $x = \ell$ and are such that the sum of forces and moments on the beam equals zero.
The material of the beam is considered to be homogenous, isotropic and linear elastic, with elasticity modulus E and Poisson ration ν.

Finally, it should be noted that Saint Venant's method does not cover the especially important category of problems in which the beam is loaded in its lateral surface. The solution of such problems is usually carried out using the *'Technical Bending Theory'*, that can provide very sufficient approximate solutions for practical beam problems. The utility of Saint Venant method can be found in the fact that it can provide accurate three-dimensional solutions in problems of Linear Elastostatics, that can be used as a point of reference and validation for the simplified approximate solutions of the Technical Bending Theory.

2.2 The Boundary Value problem

The problem can be expressed bases on the stresses, which satisfy the equilibrium equations:

$$\frac{\partial \sigma_{xx}}{\partial x} + \frac{\partial \sigma_{xy}}{\partial y} + \frac{\partial \sigma_{xz}}{\partial z} = 0, \tag{2.3}$$

$$\frac{\partial \sigma_{xy}}{\partial x} + \frac{\partial \sigma_{yy}}{\partial y} + \frac{\partial \sigma_{yz}}{\partial z} = 0, \tag{2.4}$$

$$\frac{\partial \sigma_{xz}}{\partial x} + \frac{\partial \sigma_{yz}}{\partial y} + \frac{\partial \sigma_{zz}}{\partial z} = 0, \tag{2.5}$$

and the Beltrami-Michell equations [1]

$$\nabla^2 \sigma_{xx} + \frac{3}{1+\nu} \frac{\partial^2 p}{\partial x^2} = 0, \tag{2.6}$$

$$\nabla^2 \sigma_{yy} + \frac{3}{1+\nu} \frac{\partial^2 p}{\partial y^2} = 0, \tag{2.7}$$

$$\nabla^2 \sigma_{zz} + \frac{3}{1+\nu} \frac{\partial^2 p}{\partial z^2} = 0, \tag{2.8}$$

$$\nabla^2 \sigma_{xy} + \frac{3}{1+\nu} \frac{\partial^2 p}{\partial x \partial y} = 0, \tag{2.9}$$

$$\nabla^2 \sigma_{xz} + \frac{3}{1+\nu} \frac{\partial^2 p}{\partial x \partial z} = 0, \tag{2.10}$$

$$\nabla^2 \sigma_{yz} + \frac{3}{1+\nu} \frac{\partial^2 p}{\partial y \partial z} = 0, \tag{2.11}$$

where $p = (\sigma_{xx} + \sigma_{yy} + \sigma_{zz})/3$ is the hydrostatic (or volumetric) stress.

In this section, the equilibrium equations (2.3)-(2.5) and the Beltrami-Michell equations (2.6)-(2.11) will be referred to as *'field equations'*.

The boundary conditions require the definition of the stress vector $\boldsymbol{t} = \boldsymbol{\sigma} \cdot \boldsymbol{n}$ in the external surface $\partial \mathbb{B}$ of the beam, where $\boldsymbol{n}$ is the unit vector normal to $\partial \mathbb{B}$ and pointing out of the surface. Boundary $\partial \mathbb{B}$ consists of the bases and the lateral surface of the beam.

In the base of the beam at $x = \ell$, $\boldsymbol{n} = \boldsymbol{e}_x$ and the stress vector $\boldsymbol{t}^\ell$ can be written as

$$\boldsymbol{t}^\ell(y, z) = (\boldsymbol{\sigma} \cdot \boldsymbol{e}_x)_{x=\ell} = (\sigma_{xx}\boldsymbol{e}_x + \sigma_{xy}\boldsymbol{e}_y + \sigma_{xz}\boldsymbol{e}_z)_{x=\ell}. \tag{2.12}$$

Also, the stress vector in the base $x = 0$, where $\boldsymbol{n} = -\boldsymbol{e}_x$, can be written as

$$\boldsymbol{t}^0(y, z) = -(\sigma_{xx}\boldsymbol{e}_x + \sigma_{xy}\boldsymbol{e}_y + \sigma_{xz}\boldsymbol{e}_z)_{x=0}. \tag{2.13}$$

In the lateral surface of the beam the unit vector $\boldsymbol{n}$ does not have an x component, so it can be written as $\boldsymbol{n} = n_y\boldsymbol{e}_z + n_z\boldsymbol{e}_y$, and as a result the stress vector is

$$\boldsymbol{t} = (\sigma_{xy}n_y + \sigma_{xz}n_z)\boldsymbol{e}_x + (\sigma_{yy}n_y + \sigma_{yz}n_z)\boldsymbol{e}_y + (\sigma_{yz}n_y + \sigma_{zz}n_z)\boldsymbol{e}_z. \tag{2.14}$$

As it was mentioned previously, the external loads are applied strictly on the bases of the beam, while the lateral surface is not loaded. Therefore, the mathematical formulation of

---

[1] derivation of the Beltrami-Michell equations can be found in [3]

the boundary conditions of the problem is the following:

1. in the bases $x = 0$ and $x = \ell$, the stress vectors $\boldsymbol{t}^0$ and $\boldsymbol{t}^\ell$ are defined

$$\boldsymbol{t}^0(y, z) = \hat{\boldsymbol{t}}^0(y, z) \qquad \text{and} \qquad \boldsymbol{t}^\ell(y, z) = \hat{\boldsymbol{t}}^\ell(y, z) \tag{2.15}$$

   where $\hat{\boldsymbol{t}}^0(y, z)$ and $\hat{\boldsymbol{t}}^\ell(y, z)$ are known functions

2. in the non-loaded lateral surface of the beam the stress vector becomes zero, so based on equation (2.14) the resulting relations are

$$\sigma_{xy} n_y + \sigma_{xz} n_z = 0, \tag{2.16}$$

$$\sigma_{yy} n_y + \sigma_{yz} n_z = 0, \tag{2.17}$$

$$\sigma_{yz} n_y + \sigma_{zz} n_z = 0, \tag{2.18}$$

where $\boldsymbol{n}$ is the unit vector normal to the lateral surface of the beam and pointing outside.

2.3 External loads on the bases

The total external force and moment $(\mathbf{R}^\ell, \mathbf{M}^\ell)$ on the base $x = \ell$ are applied on the geometric center O^ℓ of the cross section and have the form

$$\mathbf{R}^\ell = N\boldsymbol{e}_x + Q_y \boldsymbol{e}_y + Q_z \boldsymbol{e}_z, \qquad \mathbf{M}^\ell = T\boldsymbol{e}_x + M_y \boldsymbol{e}_y + M_z \boldsymbol{e}_z, \tag{2.19}$$

where N is the axial force, (Q_y, Q_z) are the transverse forces, T is the torsion moment and (M_y, M_z) are the bending moments.

Respectively, the loads $(\mathbf{R}^0, \mathbf{M}^0)$ on the base $x = 0$ are applied on the geometric center O^0 of the cross section and are such that the sum of all forces and moments on the beam is zero $(\mathbf{R}^\ell + \mathbf{R}^0 = \mathbf{0}$ and $\mathbf{M}^\ell + (\ell\mathbf{e}_x) \times \mathbf{R}^\ell + \mathbf{M}^0 = \mathbf{0})$. Consequently, the loads $(\mathbf{R}^0, \mathbf{M}^0)$ are equal to

$$\mathbf{R}^0 = -\mathbf{R}^\ell = -(N\boldsymbol{e}_x + Q_y \boldsymbol{e}_y + Q_z \boldsymbol{e}_z) \tag{2.20}$$

and

$$\mathbf{M}^0 = -\left[\mathbf{M}^\ell + (\ell\boldsymbol{e}_x) \times \mathbf{R}^\ell\right] = -T\boldsymbol{e}_x - (M_y - \ell Q_z)\boldsymbol{e}_y - (M_z + \ell Q_y)\boldsymbol{e}_z. \tag{2.21}$$

The mathematical problem presented in the previous paragraphs of this section, is very difficult to be defined accurately in most practical cases. More specifically, the stress vectors $\boldsymbol{t}^0(y, z)$ and $\boldsymbol{t}^\ell(y, z)$ that appear in the boundary conditions (eq.2.15), meaning the distribution of the stresses $(\sigma_{xx}, \sigma_{xy}, \sigma_{xz})$ in the bases of the beam, are practically impossible to be determined accurately. For that reason, the common approach is to use the total force and moment applied on the bases of the beam $(\mathbf{R}^\ell, \mathbf{M}^\ell, \mathbf{R}^0, \mathbf{M}^0)$ which are known quantities, instead of the exact distribution of stresses, which is very hard to define and utilize.

The beams examined in Saint Venant's theory have a length ℓ that is significantly larger than the dimensions of the cross section of the beam. In addition to that, Saint Venant's principle states that the exact distribution of stresses in the bases of the beam has a minor effect on the solution of the problem in regions located in a sufficient distance from the bases. Therefore, using the 'simpler' approach of the total load boundary conditions can still provide with accurate results for the stress distribution on the beam, without taking into account the exact stress distribution on the bases.

The Saint Venant problem with the general loads $\mathbf{R}^\ell$ and $\mathbf{M}^\ell$ shown in equation (2.19) can be solved as a superposition of the 4 elementary problems shown below:

- extension or compression of the beam with an axial (longitudinal) load N applied at the ends

- torsion of the beam with a moment T applied at the ends

- bending of the beam with moments M_y and M_z applied at the ends

- bending with transverse forces Q_y and Q_z on the base $x = \ell$, while the base $x = 0$ is loaded with forces of equal magnitude and opposite direction, and the bending moments $M_y^0 = -\ell Q_z$ and $M_z^0 = \ell Q_y$ in order to maintain the static equilibrium of the beam.

A detailed analysis of the 4 types of loads individually can be found in [4].

2.4 Bending with transverse forces
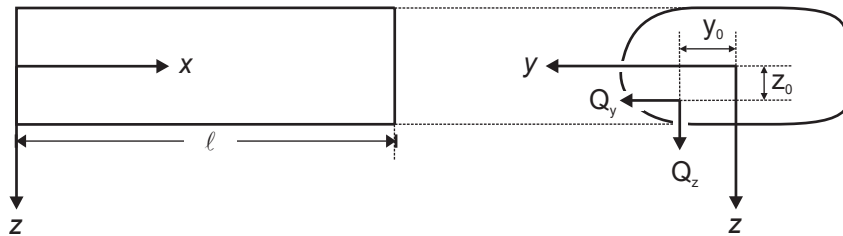
Figure 2.2: Bending of beam with transverse forces.

In this section, a central x-y-z axis system is considered (Figure 2.2) in order to analyze the problem of a bending beam. The beam is loaded with transverse bending forces Q_y and Q_z on its $x = \ell$ base, while the total moment on that base is zero as it is shown below:

$$\mathbf{R}^\ell = Q_y \boldsymbol{e}_y + Q_z \boldsymbol{e}_z \qquad \text{and} \qquad \mathbf{M}^\ell = \mathbf{0} \tag{2.22}$$

In order to maintain the static equilibrium of the beam, the corresponding total forces and moments on the base $x = 0$ are:

$$\mathbf{R}^0 = -\mathbf{R}^\ell = -Q_y \boldsymbol{e}_y - Q_z \boldsymbol{e}_z \qquad \text{and} \qquad \mathbf{M}^0 = -(\ell \boldsymbol{e}_x) \times \mathbf{R}^\ell = \ell(Q_z \boldsymbol{e}_y - Q_y \boldsymbol{e}_z). \quad (2.23)$$

The solution of the bending problem with transverse forces is complex (Sokolnikoff [6], chapter 4). For that reason there will not be a detailed proof of the solution, but rather a brief presentation of its form.

The stress field developed on the beam due to the bending forces is

$$[\boldsymbol{\sigma}] = \begin{bmatrix} \sigma_{xx}(x,y,z) & \sigma_{xy}(y,z) & \sigma_{xz}(y,z) \\ \sigma_{xy}(y,z) & 0 & 0 \\ \sigma_{xz}(y,z) & 0 & 0 \end{bmatrix} \quad (2.24)$$

The normal stress σ_{xx} varies linearly with y and z in the cross section and in a central axis system it is given by the relation

$$\boxed{\sigma_{xx}(x,y,z) = -E(\ell - x)(K_y y + K_z z)}, \quad (2.25)$$

where E is the modulus of elasticity of the material,

$$EK_y = \frac{1}{\Delta}(I_{yy}Q_y + I_{yz}Q_z), \qquad EK_z = \frac{1}{\Delta}(I_{yz}Q_y + I_{zz}Q_z), \quad (2.26)$$

$$I_{yy} = \int_\Omega z^2 \, dA, \qquad I_{zz} = \int_\Omega y^2 \, dA, \qquad I_{yz} = -\int_\Omega y\,z \, dA, \quad (2.27)$$

and

$$\Delta = I_{yy}I_{zz} - I_{yz}^2 > 0. \quad (2.28)$$

If the central axis y and z are also *principal* $(I_{yz} = 0)$, the value of the constants K_y and K_z is:

$$K_y = \frac{Q_y}{EI_{zz}} \qquad \text{and} \qquad K_z = \frac{Q_z}{EI_{yy}} \quad (2.29)$$

and in this case the normal stress σ_{xx} can be expressed as:

$$\boxed{\sigma_{xx}(x,y,z) = \frac{M_y(x)}{I_{yy}}z - \frac{M_z(x)}{I_{zz}}y}, \quad (2.30)$$

where

$$M_y(x) = -(\ell - x)Q_z \quad \text{and} \quad M_z(x) = (\ell - x)Q_y. \quad (2.31)$$

The shear stresses σ_{xy} and σ_{xz} are *independent of the axial coordinate x* and are determined by three harmonic functions $\varphi(y,z)$, $\varphi_1(y,z)$ and $\varphi_2(y,z)$ in a central axis system, as it is shown below:

$$\sigma_{xy}(y,z) = G\alpha_Q \left[\frac{\partial \varphi(y,z)}{\partial y} - z \right] + G \frac{\partial}{\partial y} \left[K_y \varphi_1(y,z) + K_z \varphi_2(y,z) \right] - G K_y \left[y^2 + \nu(y^2 - z^2) \right]$$

$$(2.32)$$

$$\sigma_{xz}(y,z) = G\alpha_Q \left[\frac{\partial \varphi(y,z)}{\partial z} + y \right] + G \frac{\partial}{\partial z} \left[K_y \varphi_1(y,z) + K_z \varphi_2(y,z) \right] - G K_z \left[z^2 + \nu(z^2 - y^2) \right]$$

$$(2.33)$$

where G is the shear modulus and α_Q is a constant with dimensions of $(length)^{-1}$, the value of which will be defined later in this section. The harmonic functions $\varphi(y,z)$, $\varphi_1(y,z)$ and $\varphi_2(y,z)$ are determined by solving three boundary value problems in the cross section of the beam. In a central axis system, the problems have the following form:

$$\nabla^2 \varphi \equiv \frac{\partial^2 \varphi}{\partial y^2} + \frac{\partial^2 \varphi}{\partial z^2} = 0 \quad \text{in the cross section,} \tag{2.34}$$

$$\frac{\partial \varphi}{\partial n} \equiv \frac{\partial \varphi}{\partial y} n_y + \frac{\partial \varphi}{\partial z} n_z = z n_y - y n_z \quad \text{in the boundary } \Gamma, \tag{2.35}$$

$$\nabla^2 \varphi_1 \equiv \frac{\partial^2 \varphi_1}{\partial y^2} + \frac{\partial^2 \varphi_1}{\partial z^2} = 0 \quad \text{in the cross section,} \tag{2.36}$$

$$\frac{\partial \varphi_1}{\partial n} \equiv \frac{\partial \varphi_1}{\partial y} n_y + \frac{\partial \varphi_1}{\partial z} n_z = \left[y^2 + \nu(y^2 - z^2) \right] n_y \quad \text{in the boundary } \Gamma, \tag{2.37}$$

$$\nabla^2 \varphi_2 \equiv \frac{\partial^2 \varphi_2}{\partial y^2} + \frac{\partial^2 \varphi_2}{\partial z^2} = 0 \quad \text{in the cross section,} \tag{2.38}$$

$$\frac{\partial \varphi_2}{\partial n} \equiv \frac{\partial \varphi_2}{\partial y} n_y + \frac{\partial \varphi_2}{\partial z} n_z = \left[z^2 + \nu(z^2 - y^2) \right] n_z \quad \text{in the boundary } \Gamma. \tag{2.39}$$

Function $\varphi(y,z)$ is independent of the loads, it depends entirely on the geometry of the cross section and has dimensions of $(length)^2$. The harmonic functions $\varphi_1(y,z)$ and $\varphi_2(y,z)$ are also independent of the loads. They depend on the geometry of the cross section and the Poisson ratio ν and have dimensions of $(length)^3$.

Finally, the value of the constant α_Q, that is involved in the solution of the shear stresses,

in given by the following expression:

$$\alpha_Q = \left[y_0 - \frac{1}{2(1+\nu)} \frac{I_{zz}S_2 + I_{yz}S_1}{I_{yy}I_{zz} - I_{yz}^2} \right] \frac{Q_z}{GJ} - \left[z_0 + \frac{1}{2(1+\nu)} \frac{I_{yy}S_1 + I_{yz}S_2}{I_{yy}I_{zz} - I_{yz}^2} \right] \frac{Q_y}{GJ} \qquad (2.40)$$

where

$$S_1 = \int_\Omega \left[y\frac{\partial \varphi_1}{\partial z} - z\frac{\partial \varphi_1}{\partial y} + y^2 z + \nu z(y^2 - z^2) \right] dA, \qquad (2.41)$$

$$S_2 = \int_\Omega \left[y\frac{\partial \varphi_2}{\partial z} - z\frac{\partial \varphi_2}{\partial y} - yz^2 + \nu y(y^2 - z^2) \right] dA, \qquad (2.42)$$

and

$$J = \int_\Omega \left(y^2 + z^2 + z\frac{\partial \varphi}{\partial y} - y\frac{\partial \varphi}{\partial z} \right) dA. \qquad (2.43)$$

Looking into equation (2.40) it can be easily concluded that the constant α_Q depends on:

- the magnitude of the loads Q_y and Q_z,

- the coordinates (y_0, z_0) of the application point of the bending force $\boldsymbol{Q} = Q_y \boldsymbol{e}_y + Q_z \boldsymbol{e}_z$,

- the shear modulus G and the Poisson ration ν of the material

- the area moments of inertia (I_{yy}, I_{zz}, I_{yz}) of the cross section

- the constant J, which depends on the geometry of the cross section, and

- the quantities (S_1, S_2), which depend on the geometry of the cross section and the Poisson ration ν.

2.5 Solution of bent beam with rectangular cross section

In this section, consider the problem of a beam bent with a transverse force. The cross section of the beam is *rectangular*. The side of the cross section parallel to the y-axis has length b and the side parallel to the z-axis has length h. The beam is loaded in the $x = \ell$ base with a force $\mathbf{R}^\ell = Q\boldsymbol{e}_z$ in the direction of the z-axis (Figure 2.3). The dimensions b and h are referred to as the 'width' and 'height' of the cross section. Due to the z-axis symmetry of the problem the constant α_Q becomes zero. Furthermore, it is

$$I_{yy} = \frac{1}{12}bh^3 \qquad\qquad I_{yz} = 0. \qquad (2.44)$$

Based on equations (2.29) it occurs that:

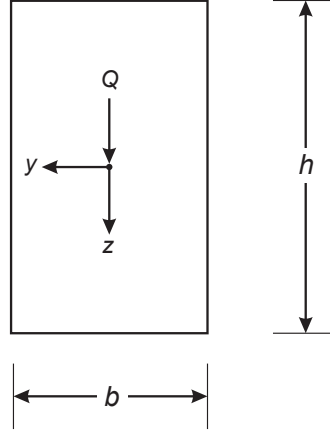$$K_y = 0, \qquad K_z = \frac{12Q}{Ebh^3}, \qquad (2.45)$$

Figure 2.3: Bending of beam with rectangular cross section.

and equation (2.25) leads to the following expression for the normal stress σ_{xx}:

$$\sigma_{xx}(x, z) = -\frac{12Q}{bh^3}(\ell - x)z = -\frac{12Q}{A}\frac{(\ell - x)z}{h^2}, \tag{2.46}$$

where $A = bh$ is the area of the cross section. The maximum value of $|\sigma_{xx}|$ is found in the positions $(x, z) = (0, \pm h/2)$:

$$|\sigma_{xx}|_{max} = \left|\sigma_{xx}\left(0, \pm\frac{h}{2}\right)\right| = \frac{6|Q|}{A}\frac{\ell}{h}. \tag{2.47}$$

Looking into equations (2.32) and (2.33) and considering the fact that the constants α_Q and K_y are zero, it becomes apparent that the effect of the harmonic functions $\varphi(y, z)$ and $\varphi_1(y, z)$ on the solution of the shear stresses is negated. Therefore, in order to obtain the solution of the shear stresses σ_{xy} and σ_{xz} it is necessary to determine the harmonic function $\varphi_2(y, z)$, by solving the following boundary value problem:

$$\nabla^2\varphi_2 = 0 \quad \text{in the cross section,} \tag{2.48}$$

$$\frac{\partial\varphi_2}{\partial n} = \left[(1 + \nu)z^2 - \nu y^2\right]n_z \quad \text{in the boundary } \Gamma \text{ of the cross section.} \tag{2.49}$$

The boundary conditions (2.49) in the sides $y = \pm b/2$ and $z = \pm h/2$ of the rectangular cross section take the following form:

$$\left.\frac{\partial\varphi_2}{\partial y}\right|_{y=\pm b/2} = 0 \quad \text{and} \quad \left.\frac{\partial\varphi_2}{\partial z}\right|_{z=\pm h/2} = (1 + \nu)\frac{h^2}{4} - \nu y^2. \tag{2.50}$$

Due to the symmetries of the problem, $\varphi_2(y, z)$ has to be an even function of y and an odd function of z. The solution of the partial differential equation is carried out utilizing the method of 'separation of variables', which suggest that $\varphi_2(y, z)$ has the following form:

$$\varphi_2(y, z) = \sum_n c_n Y_n(y) Z_n(z), \tag{2.51}$$

where every term of the infinite series satisfies the boundary conditions (2.50), Y_n are even functions of y, Z_n are odd functions of z and c_n are constants. The general solution of the Laplace equation, using the method of separation of variables, is the following:

$$\varphi_2(y, z) = c_0\, z + \sum_n \left[c_{k_n} \cos(k_n y) \sinh(k_n z) + C_{s_n} \cosh(s_n y) \sin(s_n z) \right], \tag{2.52}$$

where the only terms included are those that are even with respect to y and odd with respect to z and $(c_0, k_n, c_{k_n}, s_n, C_{s_n})$ are constants.

The boundary conditions (2.50) now take the following form:

$$\sum_n \left[-k_n c_{k_n} \sin \frac{k_n b}{2} \sinh(k_n z) + s_n C_{s_n} \sinh \frac{s_n b}{2} \sin(s_n z) \right] = 0 \quad \forall z \in \left[-\frac{h}{2}, \frac{h}{2} \right], \tag{2.53}$$

and

$$c_0 + \sum_n \left[k_n c_{k_n} \cos(k_n y) \cosh \frac{k_n h}{2} + s_n C_{s_n} \cosh(s_n y) \cos \frac{s_n h}{2} \right] = (1+\nu)\frac{h^2}{4} - \nu y^2 \quad \forall y \in \left[-\frac{b}{2}, \frac{b}{2} \right]. \tag{2.54}$$

Due to the fact that eq. (2.53) has to be true for arbitrary values of z in $-h/2 \le z \le h/2$, it occurs that $C_{s_n} = 0$ and $\sin(k_n b/2) = 0$, therefore

$$k_n = \frac{2\, n\, \pi}{b}, \qquad n = 1, 2, \ldots \tag{2.55}$$

and eq. (2.54) takes the following form:

$$c_0 + \sum_n k_n c_{k_n} \cos(k_n\, y) \cosh \frac{k_n\, h}{2} = (1+\nu)\frac{h^2}{4} - \nu\, y^2 \quad \forall\, y \in \left[-\frac{b}{2}, \frac{b}{2} \right], \tag{2.56}$$

where the constants k_n are defined in eq. (2.55). The left-hand side of equation (2.56) is the cosine Fourier series of function $(1 + \nu)\frac{h^2}{4} - \nu y^2$ in $-b/2 \le y \le b/2$.

Consequently, the constants c_0 and c_{k_n} can be calculated using the method applied in the case of Fourier series of functions. By integrating eq. (2.56) over the interval $[-b/2, b/2]$ with respect to y and taking (2.55) into consideration, the constant c_0 can be expressed as:

$$c_0 = \frac{1+\nu}{4}h^2 - \frac{\nu}{12}b^2 \,. \tag{2.57}$$

Furthermore, by multiplying eq. (2.56) with $\cos(k_m\,y)$, integrating with respect to y over $[-b/2, b/2]$ and taking (2.55) into account, the resulting expression is:

$$\sum_{n=1}^{\infty} c_{k_n} k_n \cosh \frac{k_n\,h}{2} \int_{-b/2}^{b/2} \cos(k_n\,y) \cos(k_m\,y)\,dy = -\nu \int_{-b/2}^{b/2} y^2 \cos(k_m\,y)\,dy\,. \tag{2.58}$$

Taking eq. (2.55) into account, results to

$$\int_{-b/2}^{b/2} \cos(k_n\,y) \cos(k_m\,y)\,dy = \begin{cases} 0 & (m \neq n) \\ b/2 & (m = n \neq 0) \\ b & (m = n = 0) \end{cases} \tag{2.59}$$

and

$$\int_{-b/2}^{b/2} y^2 \cos(k_m\,y)\,dy = \frac{(-1)^m}{2\,m^2\,\pi^2}\,b^3 = \frac{2\,(-1)^m}{k_m^2}\,b\,. \tag{2.60}$$

Equation (2.58) results to

$$c_{k_m}\,k_m \left(\cosh \frac{k_m\,h}{2}\right) \frac{b}{2} = -\nu\,\frac{2b\,(-1)^m}{k_m^2}\,, \tag{2.61}$$

which leads to the following expression for the constants c_{k_m}:

$$c_{k_m} = -\frac{4\,\nu\,(-1)^m}{k_m^3}\,\frac{1}{\cosh \frac{k_m\,h}{2}}\,, \qquad k_m = \frac{2\,m\,\pi}{b}\,. \tag{2.62}$$

Finally, equation (2.52) which defines $\varphi_2(y, z)$ takes the following form[2]:

$$\varphi_2(y, z) = h^3 \left\{ \frac{1}{4} \left[1 + \nu \left(1 - \frac{1}{3} \left(\frac{b}{h} \right)^2 \right) \right] \frac{z}{h} - \nu f_2(y, z) \right\} \tag{2.63}$$

where

$$f_2(y, z) = \sum_{n=1}^{\infty} A_n \sinh \frac{n\pi z}{b/2} \cos \frac{n\pi y}{b/2}$$

and the dimensionless coefficients A_n, which depend on n and the ratio b/h:

$$A_n \left(\frac{b}{h} \right) = \frac{1}{2\pi^3} \left(\frac{b}{h} \right)^3 \frac{(-1)^n}{n^3} \frac{1}{\cosh \frac{n\pi}{b/h}}\,.$$

---

[2]It is worth noting that when the Poisson ratio becomes zero ($\nu = 0$), φ_2 takes the following simple form: $\varphi_2(z) = h^2\,z/4$

By substituting the harmonic function $\varphi_2(y,z)$ defined above in equations (2.32) and (2.33), the the expressions for the shear stresses σ_{xy} and σ_{xz} are the following:

$$\sigma_{xz}(y,z) = \frac{3}{2}\frac{Q}{A}\left[1 - \left(\frac{z}{h/2}\right)^2 + \frac{\nu}{1+\nu}f_{xz}(y,z)\right], \tag{2.64}$$

$$\sigma_{xy}(y,z) = \frac{3}{2}\frac{Q}{A}\frac{\nu}{1+\nu}f_{xy}(y,z). \tag{2.65}$$

where

$$f_{xz}(y,z) = \left(\frac{y}{h/2}\right)^2 - \frac{1}{3}\left(\frac{b}{h}\right)^2 - \sum_{n=1}^{\infty}B_n\cos\frac{n\pi y}{b/2}\cosh\frac{n\pi z}{b/2}, \tag{2.66}$$

$$f_{xy}(y,z) = \sum_{n=1}^{\infty}B_n\sin\frac{n\pi y}{b/2}\sinh\frac{n\pi z}{b/2}, \tag{2.67}$$

and the dimensionless coefficients B_n, which depend on n and the ratio b/h:

$$B_n\left(\frac{b}{h}\right) = \frac{4}{\pi^2}\left(\frac{b}{h}\right)^2\frac{(-1)^n}{n^2}\frac{1}{\cosh\frac{n\pi}{b/h}}. \tag{2.68}$$

The functions f_2, f_{xz} and f_{xy} given in equations (2.63), (2.66) and (2.67) introduce the Poisson effect in the solution and they are functions of $(\frac{y}{b/2}, \frac{z}{h/2}, \frac{b}{h})$.

In the special case where the Poisson ration is zero ($\nu = 0$), the shear stresses are independent of y, the functions f_2, f_{xz} and f_{xy} do not appear in the solution and the expressions of the shear stresses take the following simple form:

$$\sigma_{xz}|_{\nu=0}(z) = \frac{3}{2}\frac{Q}{A}\left[1 - \left(\frac{z}{h/2}\right)^2\right] \quad \text{and} \quad \sigma_{xy}|_{\nu=0} = 0. \tag{2.69}$$

The distribution of σ_{xz} across the width b in the middle of the cross section ($z = 0$) is given by the following expression:

$$\sigma_{xz}(y,0) = \frac{3}{2}\frac{Q}{A}\left\{1 + \frac{\nu}{1+\nu}\left[\left(\frac{y}{h/2}\right)^2 - \frac{1}{3}\left(\frac{b}{h}\right)^2 - \sum_{n=1}^{\infty}B_n\cos\frac{n\pi y}{b/2}\right]\right\}, \tag{2.70}$$

where the coefficients B_n depend on n and the ratio b/h, defined in equation (2.68).

Figure (2.4) shows the distribution of $\sigma_{xz}(y,0)$ across the width of the cross section for various values of the ratio h/b, with $\nu = 0.3$. It is worth noting that the stress distribution depends heavily on the ratio h/b of the cross section (Reissner and Thomas [8]). The maximum value of $|\sigma_{xz}(y,0)|$ is located at the edges $y = \pm\frac{b}{2}$ while the minimum value is
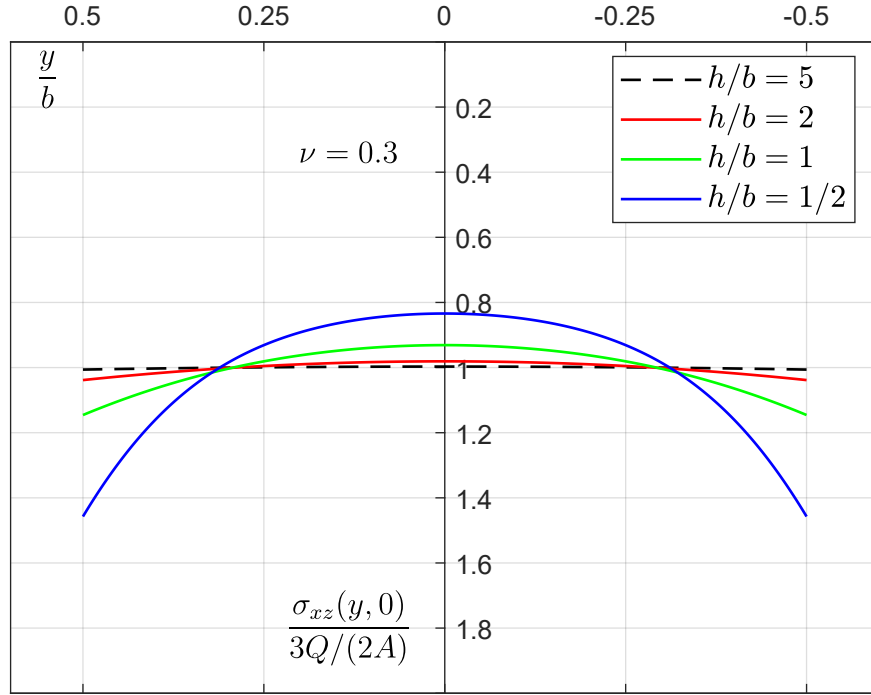
Figure 2.4: Distribution of shear stress $\sigma_{xz}(y, 0)$ in the width of the cross section for various values of h/b ratio, when Poisson ratio is $\nu = 0.3$.

found in the middle $y = 0$ of the cross section.

$$|\sigma_{xz}(y, 0)|_{max} = \left|\sigma_{xz}\left(\pm\frac{b}{2}, 0\right)\right| \qquad \text{and} \qquad |\sigma_{xz}(y, 0)|_{min} = |\sigma_{xz}(0, 0)|. \qquad (2.71)$$

When the height h is larger than two times the width b ($h > 2b$), the distribution of σ_{xz} across the width of the cross section is nearly uniform and the difference between the values at the edges and the center of the cross section at $z = 0$ is relatively small and it becomes even smaller as the h/b ration increases. On the contrary, when the height is smaller than the width ($h < b$), the difference between the values at the edges and the center of the cross section at $z = 0$ is significantly large and it becomes even larger as the h/b ration decreases.

Similar observations can be made on the distribution of the σ_{xy} stress. In this case, the maximum value of σ_{xy} is located at the 'top' and 'bottom' edges of the cross section, where $z = \pm\frac{h}{2}$. The distribution of $\sigma_{xy}(y, h/2)$ across the width at the bottom of the cross section ($z = h/2$), where the maximum value is located, is given by the following expression:

$$\sigma_{xy}(y, h/2) = \frac{3}{2}\frac{Q}{A}\frac{\nu}{1+\nu}\sum_{n=1}^{\infty} B_n \sin\frac{n\pi y}{b/2} \sinh\frac{n\pi h}{b}, \qquad (2.72)$$

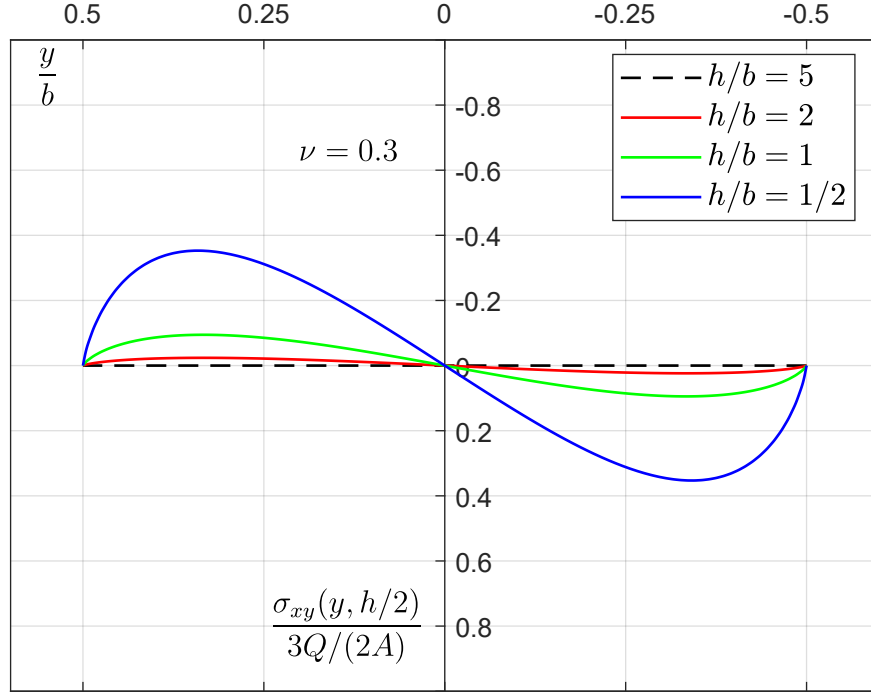with coefficients B_n defined by equation (2.68).

Figure 2.5: Distribution of shear stress $\sigma_{xy}(y, h/2)$ in the width of the cross section for various values of h/b ratio, when Poisson ratio is $\nu = 0.3$.

As it is shown in figure (2.5) the distribution of $\sigma_{xy}(y, h/2)$ across the width is significantly affected by the h/b ratio of the cross section. The maximum value of $|\sigma_{xy}(y, h/2)|$ is not located at the edges $y = \pm\frac{b}{2}$ as it was in the case of $\sigma_{xz}(y, 0)$. The position of the maximum value varies based on the h/b ration of the cross section. Further observation of the figure leads to the conclusion that σ_{xy} behaves similarly to σ_{xz}, examined in the previous paragraph. When the h/b ratio becomes larger than 2, $|\sigma_{xy}(y, h/2)|_{max}$ is relatively small and the distribution of $\sigma_{xy}(y, h/2)$ across the width tends to become uniform and equal to zero as h/b increases. When the value of h/b decreases, $|\sigma_{xy}(y, h/2)|_{max}$ becomes significantly larger. The minimum value of $|\sigma_{xy}(y, h/2)|$ is zero and it is located at the edges $y = \pm\frac{b}{2}$ and in the middle $y = 0$ of the cross section

$$|\sigma_{xy}(y, h/2)|_{min} = |\sigma_{xy}(0, h/2)| = \left|\sigma_{xy}\left(\pm\frac{b}{2}, h/2\right)\right| = 0. \qquad (2.73)$$

With regard to the maximum value of shear stresses in the entire cross section, the following remarks can be made. With the exception of certain cases, that will be mentioned afterwards, *the maximum shear stress in the cross section is σ_{xz} and it is located in the positions $(y, b) = (\pm b/2, 0)$*

$$|\sigma_{xz}(y, z)|_{max} = \left|\sigma_{xz}\left(\pm\frac{b}{2}, 0\right)\right|. \qquad (2.74)$$

An interesting exception in the location of the maximum shear stress value occurs when *the width b is roughly* 20 *times larger than the height h of the cross section* ($b > 20h$). In this case, the maximum shear stress in the cross section is the 'horizontal' shear stress σ_{xy} (normal to the direction of the bending force $\mathbf{R}^{\ell} = Q\boldsymbol{e}_z$). The maximum values are located in the 'top and bottom' sides of the cross section, meaning the positions where $z = \pm\frac{h}{2}$ and close to the corners of the rectangular cross section. For instance, when $h = b/25$ and the Poisson ratio is $\nu = 0.3$:

$$\text{in positions } (y, z) = \left(\pm 0.456\, b, \pm \frac{h}{2} \right) : \qquad |\sigma_{xy}| = 15.34 \frac{Q}{A}, \tag{2.75}$$

$$\text{in positions } (y, z) = \left(\pm \frac{b}{2}, 0 \right) : \qquad |\sigma_{xz}| = 14.00 \frac{Q}{A}. \tag{2.76}$$

Chapter 3

Finite Element Analysis Implementation

This chapter is a presentation of the steps followed in order to create a numerical model of the beam with rectangular cross section, introduced in Chapter 2. The implementation of the Finite Element Method is carried out using the 'input file' method in commercial software ABAQUS/Standard in order to create the analysis. This course of action may seem counter productive as it has a steeper learning curve, compared to using the CAE environment provided by ABAQUS, however it can be proved to be very convenient in the long term as it allows the user to make quick changes in key model parameters, assuming the file was constructed in the appropriate form. In the second part of Chapter 2 there is also a showcase of the numerical results in comparison to the analytical solution of the normal (σ_{xx}) and shear $(\sigma_{xy}, \sigma_{xz})$ stresses, that was thoroughly discussed in subsection (2.5), the approximation of which is the main purpose of this thesis.
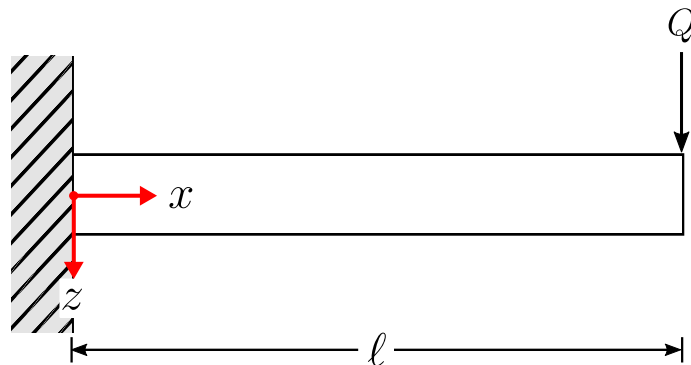
3.1 Bent Cantilever Beam Model

Figure 3.1: Schematic representation of bent cantilever beam.

3.1.1 Mesh Generation

The first major step to conduct a numerical analysis in any commercial FEA software, is to generate the geometry of the physical problem, where the spatial discretization (mesh generation) is going to take place. In the case examined in this thesis, this process involves the creation of a numerical mesh (generation of nodes and elements) that simulates a beam with rectangular cross section, with the appropriate position and orientation of a *x-y-z* axis system, in the form that was defined in the analytical solution using Saint Venant's theory (section 2.5).

Before initiating the generation of nodes and elements, it is necessary to define certain parameters. This can be achieved using ABAQUS command *PARAMETER. The primary parameters set in this section of the input file are the dimensions of the beam (length ℓ, width b etc.) and the number of elements in the x, y and z direction, which are key mesh parameters. The importance of this step lies in the fact that the input file is created in a *'parametric'* form, in the sense that the input arguments in most commands that are concerned with the mesh generation are expressed in relation to those parameters. This method of forming the input file may seem more difficult in the initial stages, but it presents significant advantages as it allows the user to make quick changes (beam dimensions, mesh density etc.) in the computational mesh and carry out the analysis right away.

In order to create the mesh, the initial step is to generate the bases of the beam. To do so, it is necessary to define the corner nodes of the cross sections $x = 0$ and $x = \ell$. The command used for that purpose is called *NODE,with input arguments that define the number and the x, y and z coordinates of the node in a fixed Cartesian coordinate system specified by ABAQUS. At this point it should be noted that the numbering of nodes (and elements) is entirely up to the user, although a good practice would be to have a systematic way of numbering, as it will be very convenient in the later stages of the analysis where sets of nodes and elements will be required in order to apply the boundary conditions of the problem. Another important remark is that the orientation and location of the beam in the *x-y-z* axis system should be the same as the one defined in the formulation of the Saint Venant problem of the beam with rectangular cross section. Therefore, the origin of the axis system should be located in the geometric center of the $x = 0$ base of the beam and the x axis should be the longitudinal axis (parallel to the lateral surface) that crosses the geometric centers of all the cross sections. To achieve that the coordinates of the corner nodes of the beam should be defined in a way that one of the bases is located in the $x = 0$ plane and the other in the $x = \ell$ plane. Arranging the axis system in this manner will result in numerical results that correspond to the analytical ones (S12 stress in Abaqus is equivalent to the σ_{xy} stress defined in the exact solution etc.). Otherwise, the user will have to transform the resulting stresses to compare them to the analytical ones, something that is inconvenient and can be avoided.

At this stage, with the corner nodes of the bases being adequately defined, the following step is to fill the two bases and ultimately the entire beam with nodes in a systematic way. This is carried out using the command *NGEN with input arguments that define the amount and

the numbering of the generated nodes. It is also important to place the generated nodes in node groups using the secondary commands NSET. Finally, using the *NFILL command in conjunction with the appropriate sets of nodes, the bases and eventually the entire beam are filled with nodes.
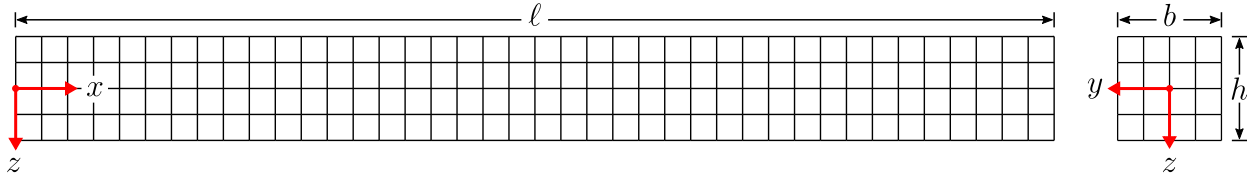

Figure 3.2: Schematic representation of computational mesh.

The mesh construction is concluded with the placement of elements in the completed node mesh, described in detail in the previous paragraphs. The command *ELEMENT is used in order to place the 'master element' in the desired position. The elements implemented for the purposes of this analysis are isoparametric, tetrahedral, 8-node continuum elements. A secondary input of the command is 'TYPE=' and it is used to specify the type of element used in the analysis. In this particular analysis the element type used is 'C3D8H'. Finally, the mesh is filled with elements using the command *ELGEN, which defines the number of elements per direction and the desired elements numbering. A detailed description of the input arguments with relevant examples can be found in the Abaqus Documentation.

3.1.2 Material Properties

Before applying the boundary conditions of the problem, it is essential to specify the material properties of the model. A necessary preliminary step is to place all the elements that are being defined in a group using the *SOLID SECTION command with the secondary parameter ELSET, set equal to the name of the element set containing these elements. The material definition process is initiated with the command *MATERIAL. Since this work is concerned with linear elastic analysis the appropriate following command is *ELASTIC. The optional parameter TYPE is used to specify the constitutive behavior of the linear elastic material and therefore, it is set to ISOTROPIC. The input arguments in *ELASTIC are the elastic constants of the material. Since the material is considered to be isotropic only two independent elastic constants are required in order to fully determine its behavior, as it was discussed in subsection (1.1.5). The constants input in this case are the Young's modulus E and the Poisson ratio ν.

3.1.3 Boundary Conditions

The second major stage of the numerical analysis is to impose the desired boundary conditions on computational mesh, which was thoroughly discussed in the previous section.

As it was stated in Chapter 1, in the case of Saint Venant beams the boundary conditions are applied at the bases of the beam, while the lateral surface is not loaded. In this analysis, the $x = 0$ end of the beam is fixed ($\boldsymbol{u} = \boldsymbol{0}$) and a concentrated load is applied at the geometric center of the $x = \ell$ base, in the z direction as it was demonstrated in the analytical solution of beams with rectangular cross section.

3.1.3.1   Kinematic BC

The $x = 0$ end of the beam, where the kinematic boundary condition is applied, is fixed using the command *BOUNDARY. The first input argument is the name of the node set, which includes the nodes of the $x = 0$ base and the second argument is 'ENCASTRE'. This option sets all the degrees of freedom of the designated nodes to zero. In this case, given the fact that the spatial discretization is carried out using continuum elements, each node has three degrees of freedom, the components of the displacement vector (u_x,u_y,u_z).

3.1.3.2   Concentrated Load BC

To apply the load boundary condition at the $x = \ell$ end of the beam a 'loading step' has to be initiated using the command *STEP. Multiple loads in an Abaqus analysis are applied in separate loading steps initiated by *STEP. In this particular analysis there is only a single loading step in which the load is applied using the command *STATIC, which defines the incrementation of the applied load. Since the analysis is linear elastic with small strains and displacements, the load is applied in a single increment without having any issues concerning the accuracy or convergence of the solution. The concentrated load (Figure 3.3) is applied using the command *CLOAD, which defines the central node of the $x = \ell$ base as the point of application as well as the direction and magnitude of the force.
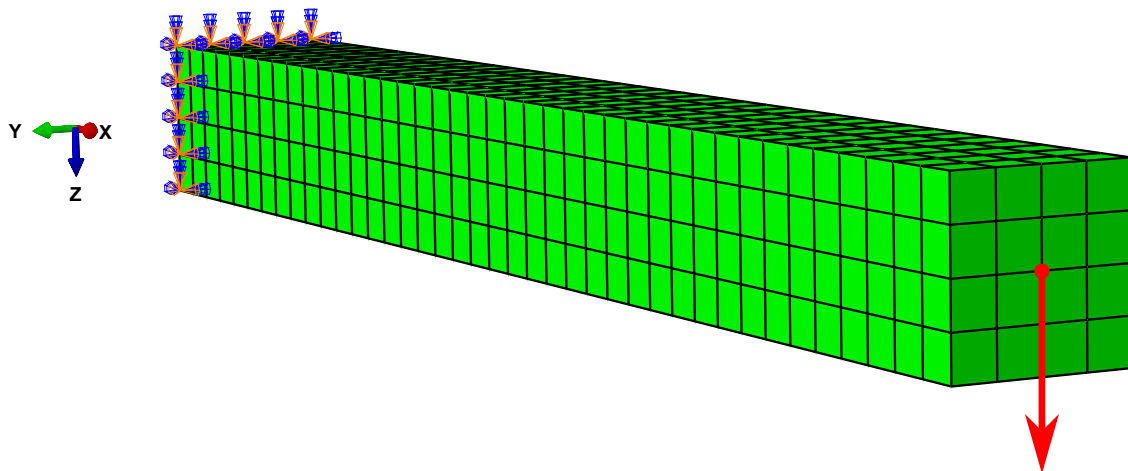

Figure 3.3: Bent cantilever beam loaded with a concentrated load on its $x = \ell$ base.

3.1.3.3 Distributed Shear Load BC

In the later stages, the analysis was carried out using an alternative load with the intention to verify 'Saint Venant's principle', as it will be discussed in the following section. For that purpose, the concentrated load, which was originally used, was replaced with a shear load uniformly distributed in the surface of the $x = \ell$ base of the beam (Figure 3.4). In order to introduce a load of this form in the analysis, it is necessary to define the surface where it is going to be applied. That can be achieved with the command *SURFACE, combined with an element set (allocated using the *ELSET command) that includes the layer of elements at the $x = \ell$ end of the beam, as well as the appropriate element face label. The face label (in this instance S5) is used to designate the faces of the elements that constitute the surface where the load is applied. This type of surface is characterized as 'element-based' in Abaqus Documentation due to the fact that an auxiliary element set was utilized to define it. Finally, the distributed shear load is applied utilizing the command *DSLOAD in conjunction with the the aforementioned surface, the keyword 'TRSHR', which declares that the requested load is a shear surface traction, and its components in the x, y and z direction.
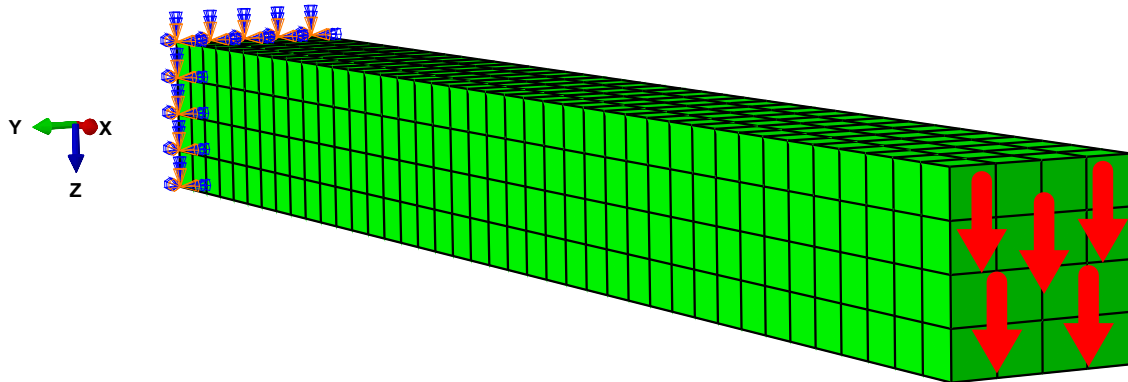

Figure 3.4: Bent cantilever beam loaded with a distributed shear load on its $x = \ell$ base.

3.1.4 Input Parameter Normalization

A good practice to follow when constructing an Abaqus analysis it to insert all the physical quantities and parameters (such as length, force, mass etc.) in a dimensionless form. This is a simple and effective method to avoid confusion concerning the measurement units of quantities during the inspection and post-processing of numerical results. The normalization is carried out utilizing a length L^*, a time t^* and a stress σ^* that can be arbitrarily defined by the user. In this particular problem all the involved parameters can be normalized using length bend stress units therefore, there is no need to define a time t^*. The following relations showcase the normalization of the width b of the cross section, the Young modulus E and

the concentrated load Q as an example:

$$\bar{b} = \frac{b}{L^*} \, , \qquad\qquad \bar{E} = \frac{E}{\sigma^*} \, , \qquad\qquad \bar{Q} = \frac{Q}{(L^*)^2\sigma^*} \, , \qquad (3.1)$$

where the bar above the symbol of a quantity is used to denote its normalized form.

3.2 Numerical Results

3.2.1 Model Description

This subsection is a brief reference to the parameteres used in the input file of the anaysis. As it was mentioned in Saint Venant's theory, the length ℓ of the beam under examination has to be significantly larger than the dimensions of the cross section. For that reason, the length of the beam is chosen to be 10 times the largest dimension of the cross section of the beam, which in this case happens to be the the width b. In this particular analysis, the primary interest is to study the distribution of shear stresses when $h/b < 1/20$. Therefore, the the h/b ration of the cross section is chosen to be $h/b = 1/25$ and the dimensions of the beam are: $\ell = 5m$, $b = 0.5m$ and $h = 0.02m$. As far as the material properties are concerned, the Young's modulus is considered to be $E = 200GPa$, the Poisson ratio is $\nu = 0.3$ and the yield strength is $\sigma_o = 250MPa$. The material properties are chosen on purpose to emulate those of construction steel used in conventional structural applications. The magnitude of the loads used in the analysis should be selected with caution, in order to ensure that the resulting stresses and displacements of the model are within the limits of linear elasticity. A good indicator in this application is the deflection δ of the tip of the cantilever beam which can be estimated using the following relation:

$$\delta = \frac{Q\ell^3}{3EI} \qquad \text{with} \qquad I = \frac{1}{12}bh^3. \qquad (3.2)$$

If the scale of magnitude of the deflection of the tip is $\delta\ O(10^{-3})$ or smaller, it is safe to assume that the strains in the model are purely elastic. The magnitude of the loads in this particular analysis is $Q = 0.001kN$ for the concentrated load and $S = 0.1kPa$ for the statically equivalent uniformly distributed shear load. It should also be noted that the normalization (Subsection 3.1.4) of the aforementioned quantities in the input file, was carried out using the arbitrary length $L = 1m$ and the yield strength of the material $\sigma_o = 250MPa$ (Table 3.1). Finally, the mesh that was utilized to extract the results that are presented in the following sections has 1000 elements in the x-direction, 100 elements in the y-direction and 10 elements in the z-direction, for a total of one million elements.

Table 3.1: Normalized input file parameters.

$\bar{E}$	ν	$\bar{\ell}$	$\bar{b}$	$\bar{h}$	$\bar{Q}$	$\bar{S}$
800	0.3	5	0.5	0.02	$4 \cdot 10^{-9}$	$4 \cdot 10^{-7}$

3.2.2 Normal Stress σ_{xx}

Figure (3.5) shows the numerical results of normal stress σ_{xx} in different regions of the beam, in comparison to the analytical solution given by relation:

$$\sigma_{xx}(x, z) = -\frac{12Q}{A} \frac{(\ell - x)z}{h^2}. \tag{3.3}$$

Equation (3.3) suggests that stress σ_{xx} is a linear function of y and z, something that can be confirmed by the numerical results. At this point, it is worth mentioning that the distribution of σ_{xx} in the x-direction (Figure 3.5 left) displays a noticeable deviation from the exact solution in positions close to the fixed $x = 0$ end of the beam. This behavior of the solution is somewhat expected, considering *Saint Venant's principle*, which states that the solution is affected in positions close to the boundary, where the boundary condition was replaced with a different one. Should be reminded that in the formulation of bending by Saint Venant, the $x = 0$ base is loaded with forces and bending moments, while in the computational model the $x = 0$ base is fixed (Subsection 3.1.3.2). This assumption is further reinforced by examining the distribution of σ_{xx} in the height of the cross section at $x = \ell/2$. In this case, the cross section is located in a sufficient distance from the $x = 0$ base for the effect of the boundary condition change to be negated. Therefore, the numerical solution is almost identical to the exact, as it is demonstrated in Figure (3.5 right).

The form of relation (3.3) also indicates that the distribution of $\bar{\sigma}_{xx}$ is independent of y which can be confirmed by the contour plot of σ_{xx} shown in figure (3.6).

3.2.3 Shear Stresses σ_{xy} and σ_{xz}

Figures (3.7) and (3.8) show the numerical results of shear stress σ_{xy} and σ_{xz} in different regions of the beam, in comparison to the analytical solution defined by equations (2.64)-(2.68). The numerical solution seems to approximate the analytical accurately, with an error of only 5-7% in the positions where the maximum values of $|\sigma_{xy}|$ and $|\sigma_{xz}|$ are located.

Additionally, the form of the relations (2.64)-(2.68) indicates that the value of σ_{xy} and σ_{xz} is independent of variable x. Therefore, the solution is uniform in the longitudinal direction x and only depends on the position of the material point on the cross section. This can be confirmed by figures (3.9) and (3.10), as the distribution of the shear stresses in different cross sections of the beam appears to be identical.
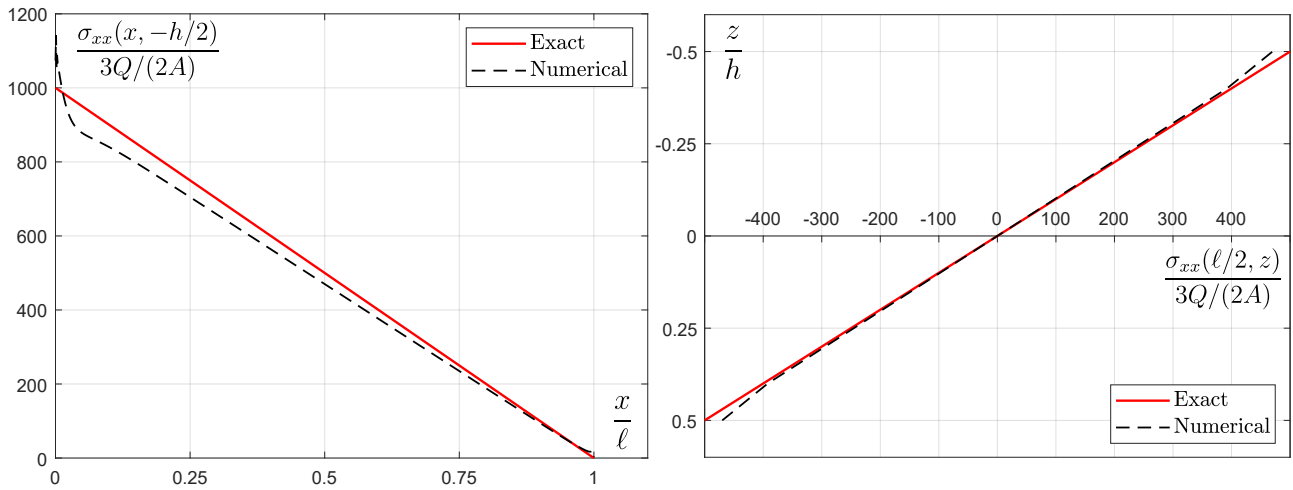
Figure 3.5: Distribution of $\sigma_{xx}(x, -h/2)$ in the longitudinal x-direction (left) and $\sigma_{xx}(\ell/2, z)$ in the height of the cross section $x = \ell/2$ (right).
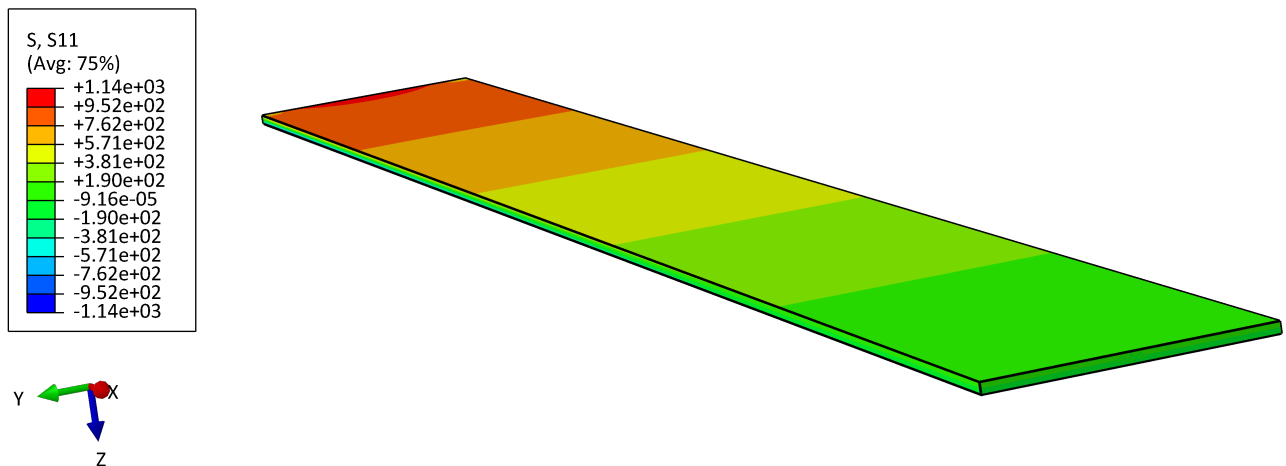

Figure 3.6: Contour plot of stress σ_{xx} (normalized with $3Q/(2A)$).

It is also worth noting that in positions close to the $x = 0$ ($0 < x < \ell/5$) and $x = \ell$ ($4\ell/5 < x < \ell$) bases of the beam, the numerical solution of the shear stresses significantly deviates from the analytical as it shown in figures (3.11) and (3.12). This can be attributed to the effect of the boundary conditions in these locations of the beam, in a similar way to the case of normal stress that was discussed in the previous subsection.

In section (2.5) certain interesting remarks were made concerning the maximum shear stress values and their location in the rectangular cross section. More specifically as it was mentioned, the distribution of shear stresses heavily depends on the h/b ratio of the cross section. In regular beam cases, such as those used in practical applications, where $h/b > 1/20$ the maximum shear stress in the cross section is σ_{xz} and it is located in the
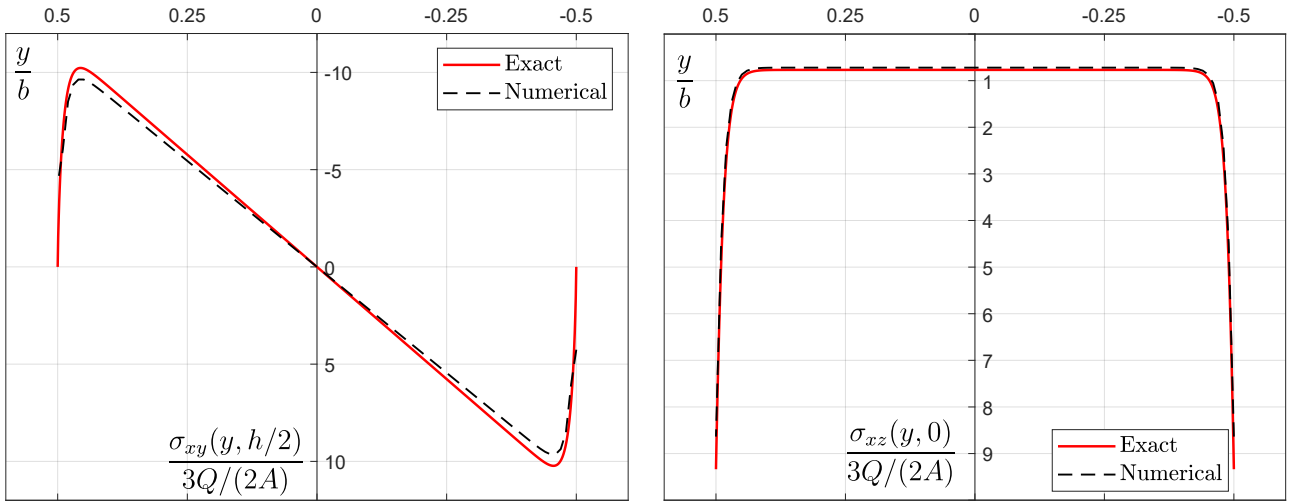
Figure 3.7: Distribution of $\sigma_{xy}(y, h/2)$ (left) and $\sigma_{xz}(y, 0)$ (right) in the width of cross section $x = \ell/2$.
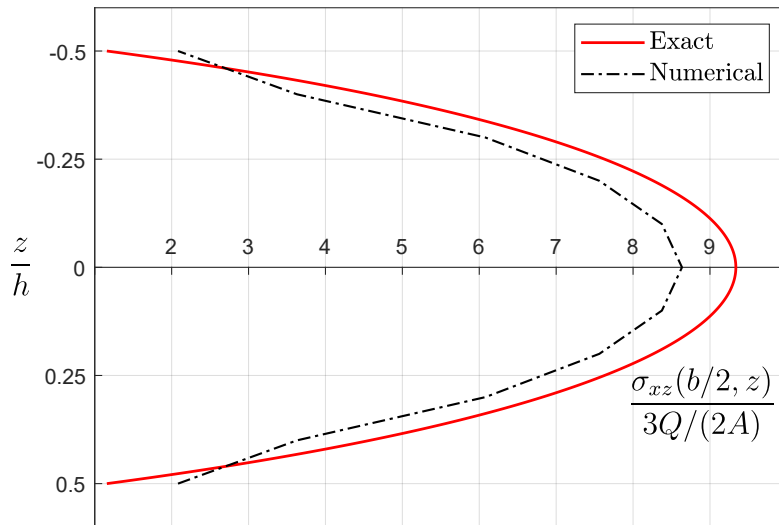

Figure 3.8: Distribution of $\sigma_{xz}(b/2, z)$ in the height of cross section $x = \ell/2$.

positions $(y, b) = (\pm b/2, 0)$:

$$|\sigma_{xz}(y, z)|_{max} = \left|\sigma_{xz}\left(\pm\frac{b}{2}, 0\right)\right|, \tag{3.4}$$

while in cases where $h/b < 1/20$, the maximum stress is σ_{xy}, with its maximum values located in the 'top and bottom' sides ($z = \pm\frac{h}{2}$) and close to the corners of the rectangular cross section.
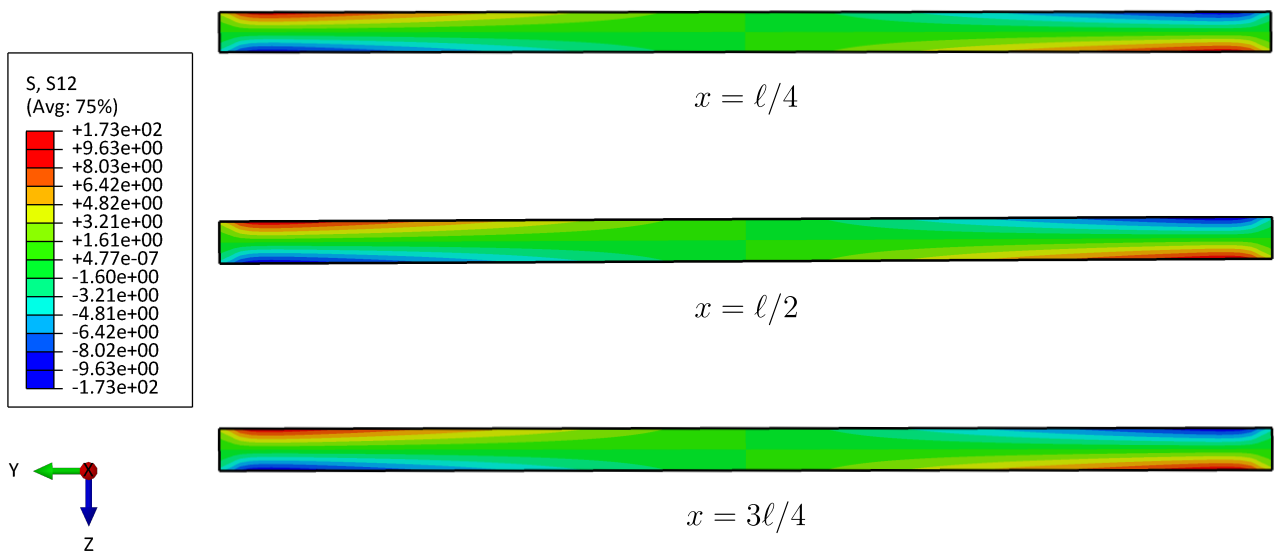
Figure 3.9: Contour plots of $\sigma_{xy}(y,z)$ in different cross sections of the beam (normalized with $3Q/(2A)$).
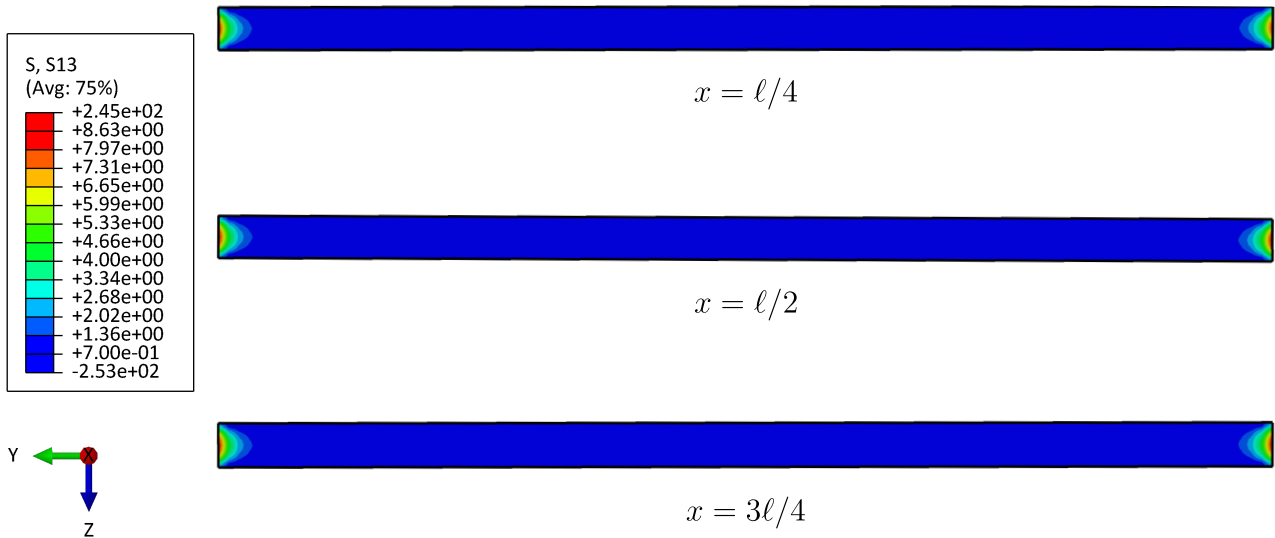

Figure 3.10: Contour plots of $\sigma_{xz}(y,z)$ in different cross sections of the beam (normalized with $3Q/(2A)$).

As it is illustrated in figure (3.13), the numerical solution is in agreement with the analytical as the maximum value of stress σ_{xy} is indeed larger than that of stress σ_{xz}, and it is located in the position it was anticipated to be, based on the exact solution.
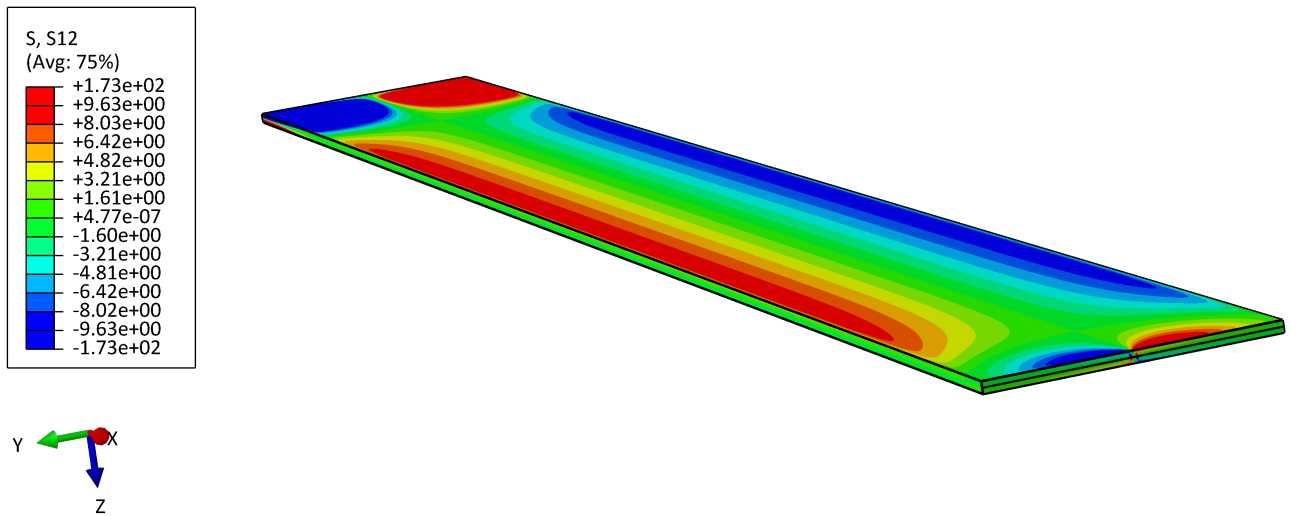
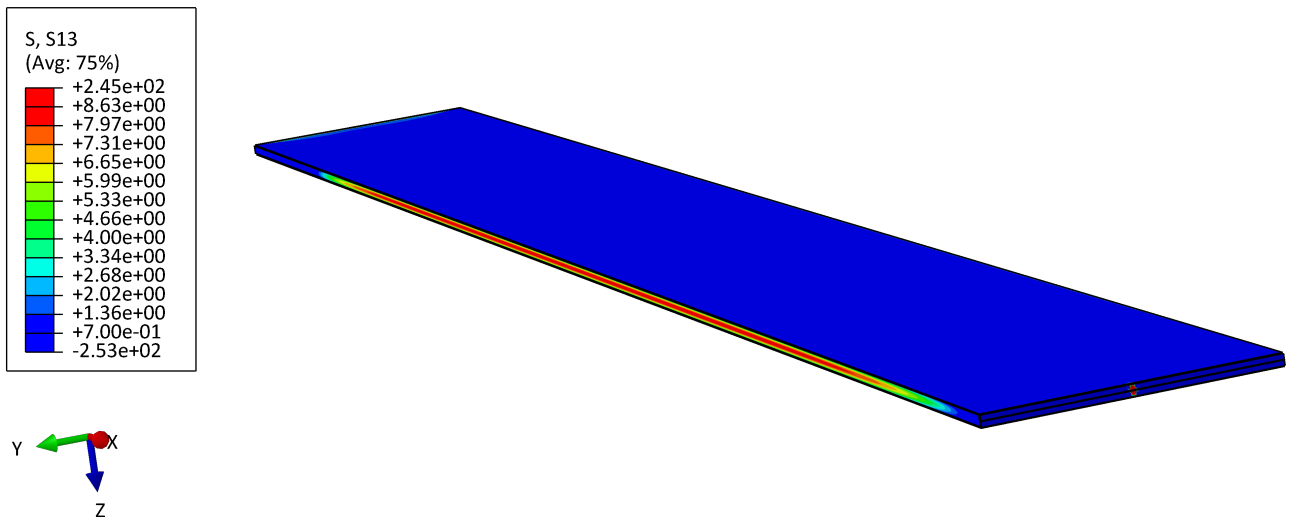Figure 3.11: Contour plots of σ_{xy} (normalized with $3Q/(2A)$).

Figure 3.12: Contour plots of σ_{xz} (normalized with $3Q/(2A)$).

3.2.4 Saint Venant's principle verification

In an attempt to verify the validity of *Saint Venant's principle*, the analysis of the bent cantilever beam is carried out with an alternative load at the $x = \ell$ base. The load used in this case is the statically equivalent, uniformly distributed shear that was discussed in subsection (3.1.3.3). The results extracted from the computational model with the modified load are identical to those of the original model, as it is shown in figure (3.14). Although this may not be something surprising, it is an exceptionally important result as it allows the engineer to ignore the exact distribution of stresses in the boundary under examination and still be able to obtain valuable and accurate stress results, in regions of the body sufficiently
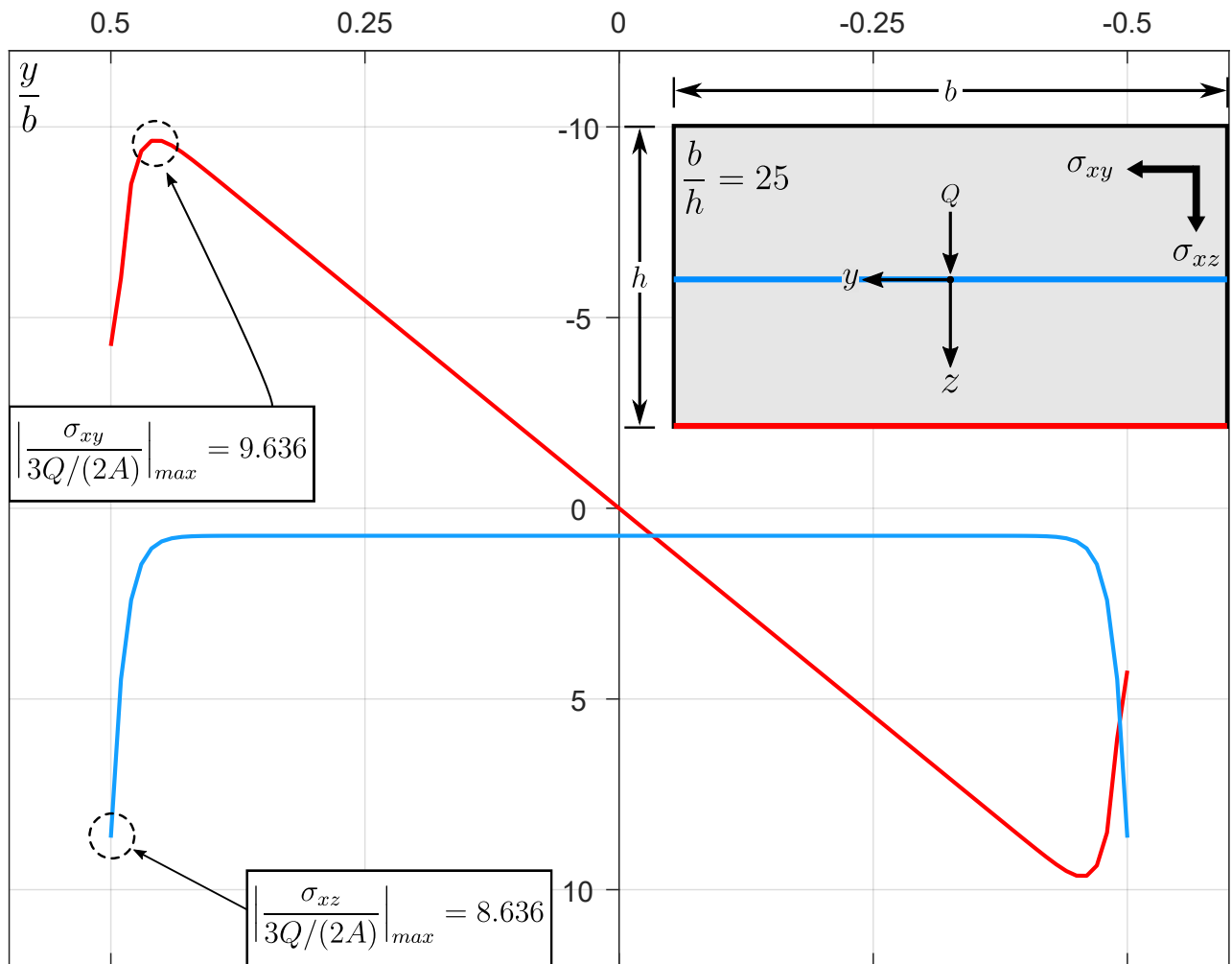
Figure 3.13: Numerical result comparison of $\sigma_{xy}(y, h/2)$ (red) and $\sigma_{xz}(y, 0)$ (blue) distributions in the width of cross section $x = \ell/2$.
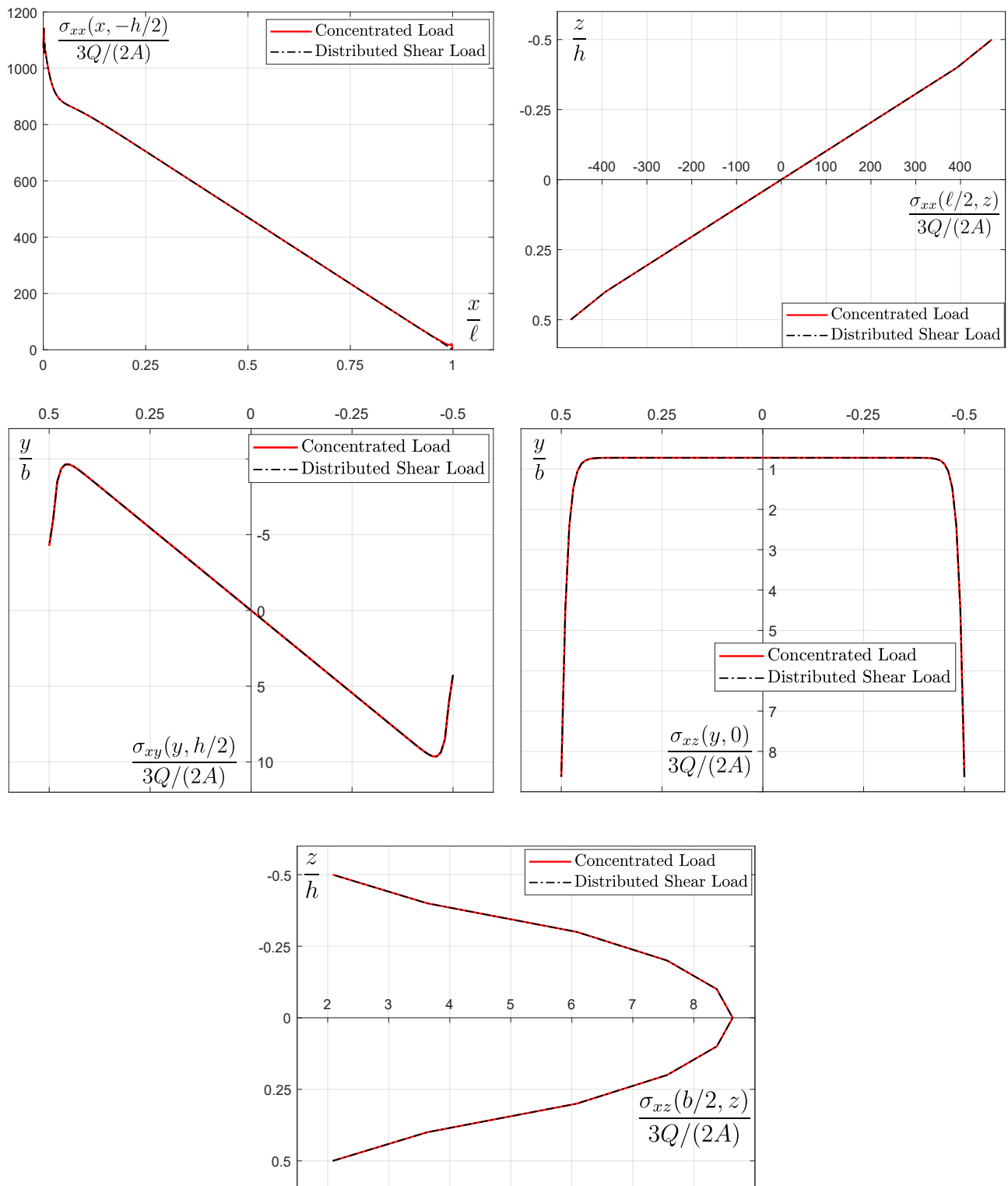
far from the boundary.

Figure 3.14: Comparison of numerical results of the two models with alternative boundary conditions.

Discussion and Conclusions

This thesis is devoted to the analysis of prismatic linear elastic isotropic beams with the intent to determine the stress field developed and study the properties of the shear stresses in relation to the geometry of the cross section, by solving the boundary value problem utilizing both analytical and computational methods.

The problem of the beam with rectangular cross section bent by transverse shear forces is solved using Saint Venant's method (Chapter 2) in order to obtain the distribution of normal (σ_{xx}) and shear stresses (σ_{xy}, σ_{xz}). The finite element method is developed using software ABAQUS in order to generate and solve the numerical model of a statically equivalent cantilever beam loaded on its $x = \ell$ base. The loads used in the model were a concentrated load applied on the central node of the $x = \ell$ base and a statically equivalent uniformly distributed shear load on the same base (Chapter 3). Examining and comparing the results that occurred by applying the aforementioned methods, the main conclusions that can be drawn are:

- The application of the finite element method using commercial softwares is well suited for the analysis of three dimensional models of beams.

- The side ratio b/h of the rectangular cross section has a significant influence on the shear stress distribution. Moreover, an interesting fact which was verified by the numerical solution is that in beams with a side ratio b/h larger than 20 the maximum shear stress in the cross section is σ_{xy} instead of σ_{xz}.

- The accuracy of the numerical results in comparison to the exact solution is remarkable.

- The modification of the boundary condition has a significant effect on the solution and causes it to deviate from the analytical in locations of the beam that are close to the boundary where the change took place.

- Saint Venant's principle is verified, considering the fact that the numerical results, which occur from the two models with the alternative types of load, are identical in locations sufficiently far from the $x = \ell$ end of the beam where the load is applied.

Bibliography

[1] ABAQUS/Standard, Version 6.14, © Dassault Systémes, 2014

[2] ABAQUS, Analysis User's Manual, Version 6.14, © Dassault Systémes, 2014

[3] Aravas N., 'Mechanics of Materials Volume I', Tziolas Publications, (2014).

[4] Aravas N., 'Mechanics of Materials Volume II: Elastic Beam Analysis', University of Thessaly Publications, (2008).

[5] Aravas N., 'Cartesian Tensors', University of Thessaly Publications, (2005).

[6] Sokolnikoff I.S., 'Mathematical Theory of Elasticity', McGraw-Hill, (1946).

[7] Mase G. T., 'Continuum Mechanics for Engineers', CRC Press, (2009).

[8] Reissner E. and Thomas G.B., 'Note on the shear stresses in a bent cantilever beam of rectangular cross section', Journal of Mathematics and Physics, vol. 25, pp. 241–243, 1946.